



HAL
open science

How glucosylation triggers physical-chemical properties of Curcumin: an experimental and theoretical study

Rois Benassi, Erika Ferrari, Sandra Lazzari, Francesca Pignedoli, Ferdinando Spagnolo, Monica Saladini

► To cite this version:

Rois Benassi, Erika Ferrari, Sandra Lazzari, Francesca Pignedoli, Ferdinando Spagnolo, et al.. How glucosylation triggers physical-chemical properties of Curcumin: an experimental and theoretical study. *Journal of Physical Organic Chemistry*, 2010, 24 (4), pp.299. 10.1002/poc.1750. hal-00599802

HAL Id: hal-00599802

<https://hal.science/hal-00599802>

Submitted on 11 Jun 2011

HAL is a multi-disciplinary open access archive for the deposit and dissemination of scientific research documents, whether they are published or not. The documents may come from teaching and research institutions in France or abroad, or from public or private research centers.

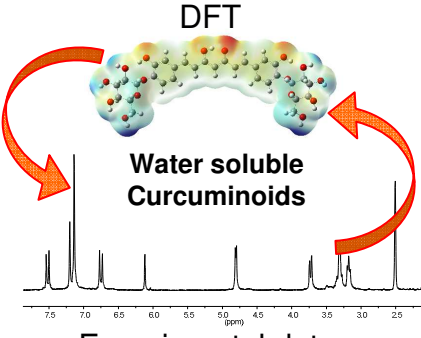
L'archive ouverte pluridisciplinaire **HAL**, est destinée au dépôt et à la diffusion de documents scientifiques de niveau recherche, publiés ou non, émanant des établissements d'enseignement et de recherche français ou étrangers, des laboratoires publics ou privés.



How glucosylation triggers physical-chemical properties of Curcumin: an experimental and theoretical study

Journal:	<i>Journal of Physical Organic Chemistry</i>
Manuscript ID:	POC-09-0283.R2
Wiley - Manuscript type:	Research Article
Date Submitted by the Author:	29-Mar-2010
Complete List of Authors:	Benassi, Rois; University of Modena and Reggio Emilia, Chemistry Ferrari, Erika; University of Modena and Reggio Emilia,, Chemistry Lazzari, Sandra; University of Modena and Reggio Emilia, Chemistry Pignedoli, Francesca; University of Modena and Reggio Emilia, Chemistry Spagnolo, Ferdinando; University of Modena and Reggio Emilia, Chemistry Saladini, Monica; University of Modena and Reggio Emilia, Chemistry
Keywords:	Curcumin, DFT, keto-enolic structure, glucosyl-curcuminoids



<p>1 A theoretical conformational 2 study on glycosyl curcuminoids is 3 performed. In order to correlate 4 their predicted spectroscopic 5 properties with IR, UV-vis and 6 NMR experimental data we 7 extended the theoretical study on 8 electronic properties in different 9 solvents (H₂O, MeOH, ACN, 10 DMSO).</p>	<p style="text-align: center;">DFT</p>  <p style="text-align: center;">Water soluble Curcuminoids</p> <p style="text-align: center;">Experimental data</p>	<p>How glycosylation triggers physical-chemical properties of Curcumin: an experimental and theoretical study</p> <p>Rois Benassi, Erika Ferrari, Sandra Lazzari, Francesca Pignedoli, Ferdinando Spagnolo and Monica Saladini</p>
--	--	---

14
15
16
17
18
19
20
21
22
23
24
25
26
27
28
29
30
31
32
33
34
35
36
37
38
39
40
41
42
43
44
45
46
47
48
49
50
51
52
53
54
55
56
57
58
59
60

For Peer Review

How glucosylation triggers physical-chemical properties of Curcumin: an experimental and theoretical study

1
2
3
4
5
6
7
8
9
10
11 Rois Benassi*, Erika Ferrari, Sandra Lazzari, Francesca Pignedoli, Ferdinando Spagnolo, Monica
12 Saladini
13
14 *Department of Chemistry, University of Modena and Reggio Emilia, via Campi 183, 41100*
15 *Modena, Italy*
16
17

18 19 Abstract

20
21 In the present study we investigate the structures of glucosylated curcumin derivatives with
22 DFT at B3LYP/6-31G* level. A conformational analysis is performed in order to determine the GS
23 (conformational minimum) and TS (rotational transition state) of curcumin derivatives and then
24 their electronic features are evaluated. HOMO and LUMO frontier orbitals and Maps of Electron
25 Density Potential (MEPs) are plotted and compared. In order to correlate their predicted
26 spectroscopic properties with IR, UV-vis and NMR experimental data we extended the theoretical
27 study on electronic properties to different solvents (H₂O, MeOH, ACN, DMSO). The main finding
28 is that the curcuminic core maintains the same geometrical and electronic structure in all
29 compounds miming the metal coordination capability showed by curcumin, therefore we may
30 confirm that the presence of glucose does not affect electronic properties of the derivatives.
31
32
33
34
35
36
37
38
39
40
41
42
43

44
45 Keywords: *Curcumin, DFT, β -keto-enolic structure, glucosyl-curcuminoids*
46
47
48
49
50
51
52
53
54
55
56
57

58
59 *Corresponding author: tel +39 0592055046, Fax +39 059373543, e-mail: rois.benassi@unimore.it
60

1. Introduction

Curcumin (1,7-bis(4-hydroxy-3-methoxyphenyl)-1,6-heptadiene-3,5-dione), a yellow spice extracted from *Curcuma Longa* L. rhizomes, is used in a wide range of applications, from industrial dyes to pharmaceutical treatments.^[1-3] It is proved that curcumin holds selective metal-chelating properties that are pharmaceutically interesting.^[4] In the field of medicinal chemistry one of the most promising properties of curcumin is its metal ligating ability towards Gallium and Iron.^[5,6] This feature can be exploited for a variety of pharmaceutical aims like metal overload detoxification, metal delivery system and radio imaging. Despite these potential pharmaceutical applications, curcumin has low water solubility and limited bioavailability that makes it difficult to handle for pharmaceutical use. To improve chemical properties of curcumin several derivatives were synthesized and studied by means of theoretical and experimental data.^[7,8] The aromatic ring glucosylation was found to enhance curcumin water-solubility and kinetic stability which is a fundamental feature for drug bioavailability.^[9] The compounds were characterized and their ability to act as metal-chelating agents was also evaluated.^[9,10] Biological properties of these molecules were also tested and they showed cytotoxicity towards human ovarian carcinoma cell line leading to an improvement of *Cisplatin* efficacy with higher selectivity towards cancer than non-cancer cells.^[11] In order to elucidate chemical-physical properties of these molecules and to correlate their electronic structures with the ability to act as metal chelating agents, in the present study we employ DFT calculations for a conformational analysis of the compounds reported in **Figure 1**. A full optimization of compounds' geometry is followed by a conformational search in order to study the potential energy surface (PES) as a function of the O-C exacyclic dihedral angle (ϕ) rotation (**Figure1**). It was reported that the presence of different solvents perturbs intra- or inter-molecular hydrogen bonds in curcumin, modifying its photophysical behavior.^[12] Therefore now we perform also a theoretical study on electronic properties of glucosyl-curcuminoids in different solvents in

1
2
3 order to correlate their predicted spectroscopic properties with IR, UV-vis and NMR experimental
4
5 data.
6
7
8
9

10 **2. Methods**

11 *2.1 Computational details*

12
13 The computations of all studied compounds were performed by DFT approach, the
14
15 structures were fully optimized using hybrid-functional B3LYP applied to 6-31G* basis set
16
17 (B3LYP/6-31G*)^[13-15] by means of Gaussian 03^[16] package of programs.
18
19

20
21 In a previous study we described curcumin structure using both B3LYP/6-311G** and
22
23 B3LYP/6-31G* levels.^[17] By comparing the obtained results, B3LYP/6-31G* showed to be a good
24
25 compromise between accuracy and precision. All the calculated properties agreed well with those
26
27 obtained using B3LYP/6-311G**. Therefore we decided to employ B3LYP/6-31G* in order to
28
29 study the influence of glucosylation on curcumin properties. GaussView 03^[18] was used as plotting
30
31 tool for data visualization.
32
33

34
35 Thermodynamics were obtained from vibrational analysis employing general procedures.
36
37 The analysis of the calculated vibrational properties always confirmed **the conformational minimum**
38
39 **(GS) or rotational transition state (TS), characterized as saddle point,** for the considered structure.
40
41

42
43 Atom charges were calculated from the optimized geometries at B3LYP/6-31G* level with
44
45 the CHELPG approach as implemented in Gaussian03. The molecular electrostatic potential maps
46
47 (MEPs) were plotted by Gaussview and reported onto 0.02 e/Bohr isosurface of electron density,
48
49 representations of HOMO and LUMO orbital density were referred to an isovalue of 0.0004.
50
51

52
53 The solvent effects were evaluated by employing the self-consistent reaction field (SCRF)
54
55 method with polarized continuum model (PCM).^[19-21]
56
57

58
59 The absorption wavelengths and oscillator strengths **were** calculated by means of time-
60
dependent density functional theory (TD-DFT) as implemented in Gaussian03. The magnetic

1
2
3 isotropic shielding tensors (σ) for ^1H and ^{13}C NMR were calculated using the standard GIAO
4
5 (Gauge-Independent Atomic Orbital) [22] at B3LYP/6-31G* approach with the Gaussian 03 program
6
7
8 package.
9

10 11 12 13 2.2 Conformational analysis

14
15 Starting with the mono glucosyl-compounds, Series A (Figure 1), all structures were fully
16
17 optimized with the DFT approach at B3LYP/6-31G* level.

18
19 We utilized the geometries of the full reoptimized structures as the starting point for a rigid
20
21 PES scan of the O-C exacyclic dihedral angle (ϕ) (Figure 1). The ϕ dihedral angle was rotated at
22
23 15° step size up to a complete 360° turn.
24
25

26
27 Minimum and maximum points on rigid PES were optimized and characterized as GS and
28
29 TS states from the vibrational analysis. For all structures the starting point was confirmed to be the
30
31 most stable structure.
32
33

34
35 Geometry of C compounds (Figure 1) was built from the more stable structure of the
36
37 corresponding A series, adding a second glucose molecule. All the possible dispositions of the
38
39 second sugar molecule with respect to curcumin planar skeleton were examined and optimized.
40
41 Calculations on C compounds were then run using the same approach (rigid PES search of ϕ
42
43 dihedral angle, optimization of the obtained structures, vibrational analysis, CHELPG charges
44
45 calculation, plots of HOMO and LUMO molecular orbitals and MEPs).
46
47
48
49

50 51 2.2 Spectroscopy

52
53 Spectroscopic data were collected only for previously synthesized compounds C.^[10]
54

55
56 NMR spectra were recorded at 300 K on a Bruker Avance AMX-400 spectrometer with a
57
58 Broad Band 5 mm probe (inverse detection). Nominal frequencies were 100.13 MHz for ^{13}C and
59
60 400.13 MHz for ^1H . The typical acquisition parameters for ^1H were as follows: 20 ppm spectral

bandwidth (SW), 6.1 μ s pulse width (90° pulse hard pulse on ^1H), 0.5-1 s pulse delay, 216-512 number of scans. For 2D H,H-Homonuclear Correlated Spettroscopy (COSY)^[23] typical parameters were used. For 2D H,X-Hetero Correlated Spettroscopy (HMBC^[24] and HMQC^[25]) oportune parameters were used ($50-90^\circ$ pulses; 32k data points; 1 s relaxation delay; 8-64k transients; $^1\text{J}_{\text{H-C}}$ 125-145 Hz; $^3\text{J}_{\text{H-C}}$ 5-15 Hz). Methanol- d_4 (MeOD) and DMSO- d_6 (DMSO) were used as NMR solvent. D_2O spectra showed line broadening due to hydrogen bond network forbidding their assignment.

UV-Vis measurements were performed using Jasco V-570 spectrophotometer at $25.0 \pm 0.1^\circ\text{C}$ in the 200-600 nm spectral range employing a 1 cm quartz cell. 2.5×10^{-5} M solutions were prepared using different solvents: H_2O , ACN, DMSO and MeOH.

The infrared spectra of solid compounds were obtained by means of a Bruker FTIR VERTEX 70, with a MCT Mid-Band detector in the $4000-600\text{ cm}^{-1}$ spectral range using an ATR Golden-Gate (Heated-Diamond top-plate).

3. Results and discussion

3.1. Conformational analysis

Previous studies^[7,17,26] demonstrated that the keto-enolic tautomer of curcumin is the most stable form, so we decided to use it to describe the core of all curcumin derivatives reported in **Figure 1**.

The first remarkable result is that for all compounds the curcuminic core maintains a completely planar conformation with the same geometrical parameters of curcumin,^[17] allowing Curcumin-like electronic conjugation of aromatic/ π electrons. This was found to be a fundamental feature to allow metal coordination through dissociated enolic moiety.^[27] The introduction of a glucose molecule may perturb curcumin skeleton by means of hydrogen bond interactions or conjugation effects, therefore we decided to scan the dihedral angle ϕ as it defines the sugar

molecule orientation. **Table 1** reports energies, thermodynamic quantities and dihedral angles (ϕ , θ) values obtained from conformational analysis of all studied compounds.

A plot of ΔG values as a function of ϕ angle for **A** type compounds is reported in **Figure 2**.

From the analysis of rotational free energy, two states of rotational maximum (TS₁ and TS₂) and two states of minimum (GS₁ and GS₂) are found.

The main differences in ϕ values are observed for the absolute minimum conformation (GS₁), ranging from 71° to 118° (**Table 1**). The ϕ value increases following the decrease of aromatic substituent steric hindrance (H<OH<OCH₃). GS₂ ground state is less influenced by substituent bulkiness, since the sugar moiety is rotated thus minimizing the interaction with the substituent on the aromatic ring (**Figure 3**). As a consequence, ϕ values in GS₂ are similar, ranging from 282° to 293°.

Free Activation Energy of rotation (ΔG^*) of TS₁ for **A2** and **A3** are similar (**A2** 7.67 Kcal mol⁻¹; **A3** 7.45 Kcal mol⁻¹), while for **A1** ΔG^* assumes an higher value (9.43 Kcal mol⁻¹). In **A1** the geometrical analysis of GS₁ (**Figure 3**) provides the evidence of an hydrogen bond between OH phenolic group and an hydroxylic oxygen atom of the sugar molecule (O33-H60...O49 1.96 Å, O-H...O angle 158.6°). The hydrogen bond breakage in **A1** strongly contributes to the higher ΔG^* . In **A2** and **A3** only steric effects are responsible for the ΔG^* value and no evidence of significant H-bond is observed. Previous study on similar β -diketo-mono-glucosylated derivatives^[27] showed the formation of an hydrogen bond involving OCH₃ aromatic substituent and glucosydic moiety (OH...O 2.23 Å, OHO angle 155°). Instead in **A2** no hydrogen interaction is observed suggesting that the greater extent of π delocalization with respect to the previously studied compound, probably makes OCH₃ group less capable to form hydrogen bond.

In di-glucosylated **C** compounds all the possible dispositions of the two sugar molecules with respect to the planar skeleton of curcumin were optimized and the results for **C2** are reported

1
2
3 in **Figure 4**, **C1** and **C3** show the same trend. The *sin-sin* configuration is the most stable therefore
4
5 it is used as the starting point for conformational analysis on ϕ dihedral angle. For all **C** compounds
6
7 the value of θ dihedral angle results close to the corresponding ϕ angle in GS_1 state of **A** compound
8
9 with opposite sign.
10
11

12
13 **C** compounds show the same trend as mono-glucosylated (**A** series) regarding PSE. The
14
15 ΔG^* and dihedral angles for **A** and **C** homologues are superimposable with a maximum difference
16
17 of $\pm 2^\circ$ (**Table 1**).
18
19

20 For each **C** compound, in all states of **maximum** and **minimum**, the value of the not scanned
21
22 θ dihedral angle is constant and equal to the ϕ value obtained in the ground state (GS_1) with
23
24 opposite sign. This evidence suggests that the two sugar molecules rotate independently and do not
25
26 influence each other during the rotation. We suggest that θ angle can rotate with the same potential
27
28 energy of ϕ since **C** compounds maintain the same symmetric structure observed in curcumin. For
29
30 all compounds the relatively low ΔG^* values ($<10.04 \text{ kcal mol}^{-1}$) allow a “free” rotation of the
31
32 glucosydic group around ϕ and θ dihedral angle at room temperature. Anyway the free rotation of
33
34 the **glucose** moieties **does** not exert any steric hindrance on keto-enolic group in any conformation,
35
36 maintaining it accessible to a metal ion for the coordination reaction.
37
38
39
40

41 We observed also the formation of an hydrogen bond interaction between OH phenolic
42
43 group and sugar molecule (O33-H82...O56 1.96 Å, O-H...O angle 158.7°) **in C1**. In a previous
44
45 study on **C** compounds we **discovered** that the nature of *meta* substituent on the aromatic ring
46
47 affects lipophilicity in the order $\text{OH} > \text{H} > \text{OCH}_3$ ^[10] Today computational data may account for the
48
49 unexpected increased lipophilicity of **C1** due to the formation of the intra-molecular hydrogen bond
50
51 **interactions** with the glucosydic moiety.
52
53
54
55
56
57
58
59
60

3.2. Molecular Orbitals

HOMO and LUMO molecular orbitals were calculated for both GS and TS conformers for **A** and **C** series. **Figure 5** shows HOMO and LUMO molecular orbitals at the GS₁ conformation, HOMO and LUMO for the other conformations GS₂, TS₁, TS₂ are perfectly overlapping with GS₁. HOMO and LUMO are delocalized through the whole curcuminic core, allocating the electron density both on the dienic and benzenic moieties as found for curcumin.^[17,26] The introduction of one or two glucose molecules does not raise any interaction between the newly attached substituent and aromatic groups, thus not affecting the peculiar conjugation of aromatic/ π electrons of curcumin core confirming the results of conformational analysis.

3.3 MEPs

Figure 6 shows the MEPs of GS₁ state. In all compounds, the negative charge of the curcuminic core is located on the β -keto-enolic oxygen atoms, resembling the same trend of curcumin.^[17,26] **Table 2** reports charge density values of β -keto-enolic and phenolic oxygen atoms of **A1** and **C1** in GS₁ state. By comparing the values obtained in *vacuum* with those of curcumin we can observe variation of ≈ 0.004 in the negative charge of the β -keto-enolic oxygen atoms, thus suggesting the same potential metal coordination ability of curcumin.^[6] The presence of OH groups in **A1** and **C1** introduces a further center of negative charge that might affect physical-chemical properties. Although enolic and phenolic *oxygens* show almost the same negative charge values the involvement of phenolic oxygen in metal coordination is prevented by the higher pK_a value [pK_a (phenolic) 9.4; pK_a (enolic) 8.2].^[11] The negative charge on OH aromatic substituent evidences its strong electron withdrawing ability, which probably influences the pK_a value of the β -keto-enolic group, in fact **C1** was found to be the most acidic compound in aqueous solution and the more effective Fe(III) and Ga(III) chelating agent.^[11]

A and **C** compounds show the same electronic properties (MEPs, CHELPG) suggesting similar coordination ability, therefore the analysis of solvent effects is limited to **C** compounds in

1
2
3 order to compare their electronic properties with experimental data. MEPs calculated in different
4 solvents look like those in *vacuum*; the corresponding density charge values are reported in **Table 2**.
5
6

7
8 We can observe a general increase of the negative charge on ketonic oxygen atom in solvent
9 with respect to *vacuum*. This effect seems to be directly related to solvent polarity, in fact H₂O
10 gives major increase in negative charge. On the contrary the ability to form hydrogen bonds seems
11 not to influence charge distribution. The high charge density on enolic function may account for the
12 replacement of hydrogen atom by metal ion with a lower pK_a value with respect to free ligand
13 system, enabling metal coordination and preventing hydroxide precipitation.
14
15
16
17
18
19
20
21

22 MEPs do not take into account higher electrostatic effects as polarization which may be very
23 important in metal complexation. Anyway the higher charge density on keto-enolic group with
24 respect to sugar oxygen atoms suggests that the keto-enolic function is the only potentially involved
25 in metal coordination. In addition chelating effect and enolic proton acidity enforces this
26 assumption. Previous NMR study on **C** compounds ^[9] established that sugar moiety was never
27 involved in metal ligation as no ¹H and ¹³C chemical shifts were observed upon metal addition.
28
29
30
31
32
33
34
35
36
37
38

39 3.3 NMR spectroscopy

40 ¹H and ¹³C NMR spectra were recorded for **C** compounds and were compared with the
41 calculated values. **Figure 7** reports ¹H NMR spectrum of **C1** in DMSO-*d*₆. Experimental data
42 evidence only one set of signals corresponding to the keto-enolic form; the complete symmetry
43 (C_{2v}) of the molecule, due to resonance between the two possible keto-enolic limit structures, is
44 supported by the equivalence of double bonds and aromatic rings, and by ¹³C NMR spectrum giving
45 undistinguishable and equivalent peaks for ketonic and enolic carbons. **C2** and **C3** behave the same.
46
47
48
49
50
51
52
53
54
55
56
57
58
59
60
The fit between experimental chemical shifts of glucosyl-curcuminoids in DMSO and MeOD for
both ¹H (**Figure 8A**) and ¹³C (**Figure 9B**) illustrates very small variation due to experimental
conditions.

The GIAO (Gauge-Independent-Atomic-Orbitals) isotropic magnetic shielding tensors (σ_{calc}) were calculated for **C1**, **C2** and **C3** in *vacuum*, H₂O, MeOH, and DMSO (**Table 1-3**, supplementary material). Bearing in mind the experimental molecular symmetry of glucosyl-curcuminoids, the average value of σ_{calc} ($\bar{\sigma}_{calc}$) between the two keto-enolic limit structures was calculated and reported in **Table 3** for each solvent system.

¹³C and ¹H experimental chemical shift assignments were supported by 2D COSY, HSQC and HMBC experiments, data are reported in **Table 4** and **Table 5**.

Plotting the experimental ¹³C and ¹H chemical shifts (δ_{exp}) in MeOD and DMSO *versus* the $\bar{\sigma}_{calc}$ in *vacuum* or in the same solvent system, a linear regression is observed: $\delta_{exp} = a \cdot \bar{\sigma}_{calc} + b$ (a, b and R² parameters are given in **Table 4** and **Table 5**). This relationship is then used to predict the chemical shifts (δ_{pred}).^[17,28] As already observed,^[29] the correlation between experimental chemical shifts and calculated isotropic screening constants is better for ¹³C than for ¹H, in fact the correlation coefficient R² ranges from 0.9834 to 0.9939 for ¹³C and from 0.9186 to 0.9718 for ¹H.

A comparison with previously reported Curcumin predicted ¹³C NMR data^[18] highlights how for glucosyl-curcuminoids the presence of the sugar moiety experiences the solvent effect, in fact linear regressions are definitely better when calculated on the basis of $\bar{\sigma}_{calc}$ in the same solvent system than *in vacuum*.

¹H δ_{pred} values (**Table 5**) have good correlation with δ_{exp} with exception of H-1, due to the fact that the GIAO σ_{calc} has almost the same value in the two resonance limit structures of keto-enolic moiety, as a consequence electronic delocalization can't be predicted accurately. **Table 5** data confirm the importance of solvent environment in predicting correct ¹H δ_{pred} , in fact the gap in R² value between *in vacuum* and solvent prediction is higher for ¹H (0.0117-0.0319) than ¹³C (0.0003-0.0044).

1
2
3 ΔR^2 values ($R^2_{\text{solvent}} - R^2_{\text{vacuum}}$) prove that solvent has a greater effect in **C1** and **C2** than in
4
5
6 **C3**; ^1H NMR data of **C1** are better predicted in MeOH than in DMSO, **C3** behaves in the opposite
7
8 way while for **C2** the two solvents show the same effect. This behavior suggests that the presence of
9
10 OH and OCH_3 group in **C1** and **C2** respectively may interact with solvent through hydrogen bond
11
12 and/or dipolar interactions.

13
14
15 **Figure 9** reports the plotting of ^1H and ^{13}C δ_{exp} vs. $\bar{\sigma}_{\text{calc}}$ for **C1** together with the linear
16
17 relationships. **C1** behaves differently from **C2** and **C3** as it concerns anomeric proton (H-11), in fact
18
19 this proton is not well predicted by calculation as a consequence of the intra-molecular hydrogen
20
21 bond between the OH phenolic group and the sugar moiety.
22
23
24
25
26

27 3.4. UV-Vis spectroscopy

28
29
30 Each compound shows a strong intense absorption band in the 300-500 nm wavelength
31
32 region. Absorption maxima are reported in **Table 6** together with calculated values in the
33
34 corresponding solvent. The red shift in DMSO with respect to ACN medium follows the order
35
36 **C1**>**C2**>**C3** and **it** is related to the higher polarity of the phenolic substituent (OH > OCH_3 > H)
37
38 interacting with different polar solvent. A solvent dependent red shift in maximum was found also
39
40 in curcumin ^[12] and was related to solvent polarity and proticity, in fact methanol, a strong
41
42 hydrogen bond-donating as well as hydrogen bond accepting gave the greatest maximum red shift.
43
44 In our case the three compounds in H_2O and MeOH behaves similarly, probably because the
45
46 hydrogen bond effect is masked by the presence of sugar moiety. The same trend is observed in
47
48 predicted values.
49
50
51
52

53 3.5 Infra Red Spectroscopy

54
55
56 Usually the calculated harmonic vibrational wavenumbers are higher than the experimental
57
58 ones, because of the anharmonicity, incomplete treatment of electron correlation and use of finite
59
60

1
2
3 one-particle basis set.^[29] A linear relationship with a good correlation coefficient is obtained
4
5 plotting the experimental wavenumbers *versus* the calculated ones ($\bar{\nu}_{\text{calc}}$) for all C compounds;
6
7
8 **Figure 10** reports C1 data. This result suggests that the over-estimation of calculated wave numbers
9
10 is quite systematic and allows to predict FT-IR spectra. The slope of the linear regression (a=
11
12 0.9991) is greater than the value (0.9613) estimated at B3LYP/6-31G* level for a great number of
13
14 different compounds.^[30] A list of the experimental and calculated frequencies together with a
15
16 tentative assignment is reported as supplementary material (Table 4 supplementary material)
17
18
19
20
21

22 Conclusions

23
24
25 We have demonstrated that the addition of bulky sugar molecule **does** not affect
26
27 electronic properties of curcuminic core,^[30] allowing metal coordination through keto-enolic moiety.
28
29 Glucose molecule interacts only with meta-substituent on aromatic ring influencing lipophilicity.
30
31

32 Solvent effect is a critical aspect in predicting spectroscopic data which well agree with
33
34 experimental ones.
35
36
37
38

39 Acknowledgments

40
41 We are thankful to the “Consorzio Interuniversitario per il Calcolo Automatico dell'Italia
42
43 Nord Orientale - CINECA” and to the “Laboratorio di Calcolo Scientifico Avanzato
44
45 Interdipartimentale dell'Università degli Studi di Modena e Reggio Emilia” for computing facilities.
46
47 We are grateful to the “Centro Interdipartimentale Grandi Strumenti – C.I.G.S.” of the University of
48
49 Modena and Reggio Emilia and to the “Fondazione Cassa di Risparmio di Modena” for supplying
50
51 NMR spectrometer.
52
53
54
55
56
57
58
59
60

References

1. S. Goel, B. Jhurani, B. Aggarwal, *Mol. Nutr. Food Res.* **2008**; 52, 1010.
2. R.A. Sharma, A.J. Gescher, W.P. Steward, *Eur. J. Cancer* **2005**; 4, 1955.
3. R.K. Maheshwari, A.K. Singh, J. Gaddipati, R.C. Srimal, *Life Sci.* **2006**; 78, 2081.
4. L. Shen, H.F. Ji, *Spectrochim. Acta A Mol. Biomol. Spectrosc.* **2007**; 67,619.
5. Y. Jiao, J. Wilkinson IV, X. Di, W. Wang, H. Hatcher, N.D. Kock, R. D'Agostino Jr, M.A. Knovich, F.M. Torti, S.V. Torti, *Blood* **2009**; 113 462.
6. M. Borsari, E. Ferrari, R. Grandi, M. Saladini, *Inorg. Chim. Acta* **2002**; 328, 61.
7. P. Cornago, R.M. Claramount, L. Bouissane, I. Alkorta, J. Elguero, *Tetrahedron* **2008**; 8089.
8. V. Bertolasi, V. Ferretti, P. Gilli, X. Yao, C. J. Li, *New J. Cem.* **2008**; 32, 694.
9. B. Arezzini, M. Ferrali, E. Ferrari, R. Grandi, S. Monti, M. Saladini, *Eur. J. Inorg. Chem.* **2004**; 3, 646.
10. E. Ferrari, B. Arezzini, M. Ferrali, S. Lazzari, F. Pignedoli, F. Spagnolo, M. Saladini, *BioMetals* **2009**; 22, 701.
11. E. Ferrari, S. Lazzari, G. Marverti, F. Pignedoli, F. Spagnolo, M. Saladini, *Biorg. Med. Chem.* **2009**; 17, 3043.
12. S.M. Khopde, K.I. Priyadarsini, D.K. Palit, T. Mukherjee, *Photochem. Photobiol.* **2000**; 72 , 625.
13. B. Miehllich, A. Savin, H. Stoll, H. Preuss, *Chem. Phys. Lett.* **1989**; 157, 200.
14. W. Lee, R. Yang, G. Parr, *Phys. Rev.* **1988**; B 37, 785.
15. A.D. Becke, *J. Chem. Phys.* **1993**; 98, 5648.
16. M.J. Frisch, G.W. Trucks, H.B. Schlegel, G.E. Scuseria, M.A. Robb, J.R. Cheeseman, J.A. Montgomery Jr., T. Vreven, K.N. Kudin, J.C. Burant, J.M. Millam, S.S. Iyengar, J. Tomasi, V. Barone, B. Mennucci, M. Cossi, G. Scalmani, N. Rega, G.A. Petersson, H. Nakatsuji, M. Hada, M. Ehara, K. Toyota, R. Fukuda, J. Hasegawa, M. Ishida, T. Nakajima, Y. Honda, O. Kitao, H. Nakai,

- 1
2
3 M. Klene, X. Li, J.E. Knox, H.P. Hratchian, J.B. Cross, V. Bakken, C. Adamo, J. Jaramillo, R.
4
5 Gomperts, R.E. Stratmann, O. Yazyev, A.J. Austin, R. Cammi, C. Pomelli, J.W. Ochterski, P.Y.
6
7 Ayala, K. Morokuma, G.A. Voth, P. Salvador, J.J. Dannenberg, V.G. Zakrzewski, S. Dapprich,
8
9 A.D. Daniels, M.C. Strain, O. Farkas, D.K. Malick, A.D. Rabuck, K. Raghavachari, J.B. Foresman,
10
11 J.V. Ortiz, Q. Cui, A.G. Baboul, S. Cliord, J. Cioslowski, B.B. Stefanov, G. Liu, A. Liashenko, P.
12
13 Piskorz, I. Komaromi, R.L. Martin, D.J. Fox, T. Keith, M.A. Al-Laham, C.Y. Peng, A.
14
15 Nanayakkara, M. Challacombe, P.M.W. Gill, B. Johnson, W. Chen, M.W. Wong, C. Gonzalez, J.A.
16
17 Pople, *Gaussian 03*, Revision C.02, Gaussian, Inc., Wallingford, CT, **2004**.
18
19
20
21
22 17. R. Benassi, E. Ferrari, S. Lazzari, F. Spagnolo, M. Saladini, *J. Mol. Struct.* **2008**; 892, 168.
23
24 18. R. Dennington II, T. Keyth, J. Millam, K. Eppinnett, W.L. Hovell, R. Gilliland, *Gaussview*,
25
26 *Version 3.0*, Semichem, Inc., Shawnee Mission, KS, **2003**.
27
28
29 19. S. Miertus, E. Scrocco, J. Tomasi, *Chem. Phys.* **1981**; 55, 117.
30
31 20. S. Miertus, J. Tomasi, *Chem. Phys.* **1982**; 65, 239.
32
33 21. M. Cossi, V. Barone, Cammi, J. *Chem. Phys. Lett.* **1996**; 255, 327.
34
35 22. K. Wolinski, J.F. Hinton, P.J. Pulay, *J. Am. Chem. Soc.* **1990**; 112, 8251.
36
37 23. K. Nagayama, A. Kumar, K. Wuethrich, R.R. Ernst, *J. Magn. Res.* **1980**; 40, 321.
38
39 24. A. Bax, M.F. Summers, *J. Am. Chem. Soc.* **1986**; 108, 2093.
40
41 25. A. Bax, R. H. Griffey, B. L. Hawkins, *J. Magn. Res.* **1983**; 55, 301.
42
43 26. E. Benassi, F. Spagnolo, *Theor. Chem. Acc.* **2009**; 124, 235.
44
45 27. R. Benassi, E. Ferrari, R. Grandi, S. Lazzari, M. Saladini, *J. Inorg. Biochem.* **2007**; 101, 203.
46
47 28. Blanco, I. Alkorta, J. Elguero, *Magn. Res. Chem* **2007**; 45, 797.
48
49 29. F. M. Szafran, E. Bartoszak-Adamska, J. Koput, Z. Dega-Szafran, *J. Mol. Struct.* **2007**; 140,
50
51 844.
52
53 30. J.B. Foresman, A. Frisch, "Exploring Chemistry with Electronic Structure Methods: A Guide
54
55 to Using Gaussian"(2 ed.), Gaussian, Inc, Pittsburgh, PA **1996**.
56
57
58
59
60

Table 1- θ and ϕ dihedral angles, total electronic energies (E), zero point vibrational energies (E + ZPE), thermodynamic quantities (G, H) and relative differences calculated at B3LYP/6-31G*.

a) Not rotated dihedral angle; b) rotated dihedral angle; c) a.u. ; d) Kcal mol⁻¹

State	θ^a	ϕ^b	E ^c	E+ZPE ^c	H ^c	G ^c	ΔE^d	$\Delta E+ZPE^d$	ΔH^d	ΔG^d
A1 GS ₁	-	99.89	-1795.689556	-1795.202059	-1795.166855	-1795.272771	0.00	0.00	0.00	0.00
TS ₁	-	203.03	-1795.675170	-1795.188357	-1795.153763	-1795.257743	9.03	8.60	8.22	9.43
GS ₂	-	282.23	-1795.685569	-1795.198340	-1795.162987	-1795.269849	2.50	2.33	2.43	1.83
TS ₂	-	358.46	-1795.675225	-1795.188406	-1795.153778	-1795.257568	8.99	8.57	8.21	9.54
A2 GS ₁	-	71.35	-1874.295775	-1873.750883	-1873.712800	-1873.826631	0.00	0.00	0.00	0.00
TS ₁	-	216.94	-1874.286710	-1873.742105	-1873.704899	-1873.814405	5.69	5.51	4.96	7.67
GS ₂	-	293.57	-1874.293078	-1873.747762	-1873.709895	-1873.822106	1.69	1.96	1.82	2.84
TS ₂	-	347.61	-1874.288686	-1873.744054	-1873.706854	-1873.816857	4.45	4.29	3.73	6.13
A3 GS ₁	-	117.93	-1645.248964	-1644.770062	-1644.737057	-1644.839474	0.00	0.00	0.00	0.00
TS ₁	-	215.56	-1645.238652	-1644.760269	-1644.728023	-1644.827595	6.47	6.15	5.67	7.45
GS ₂	-	285.75	-1645.247768	-1644.768673	-1644.735734	-1644.838272	0.75	0.87	0.83	0.75
TS ₂	-	354.04	-1645.240588	-1644.762127	-1644.729889	-1644.829315	5.26	4.98	4.50	6.37
C1 GS ₁	-100.42	100.33	-2406.423034	-2405.761907	-2405.715397	-2405.848672	0.00	0.00	0.00	0.00
TS ₁	-100.76	203.85	-2406.408721	-2405.748111	-2405.702281	-2405.832897	8.98	8.66	8.23	9.90
GS ₂	-100.38	283.45	-2406.419166	-2405.757980	-2405.711444	-2405.843949	2.43	2.46	2.48	2.96
TS ₂	-101.45	358.72	-2406.408670	-2405.748086	-2405.702199	-2405.832666	9.01	8.67	8.28	10.04
C2 GS ₁	-70.29	70.21	-2485.008984	-2484.291502	-2484.241500	-2484.383139	0.00	0.00	0.00	0.00
TS ₁	-69.85	216.44	-2484.999813	-2484.282656	-2484.233480	-2484.372251	5.75	5.55	5.03	6.83
GS ₂	-70.32	292.82	-2485.005972	-2484.288132	-2484.238297	-2484.379928	1.89	2.11	2.01	2.01
TS ₂	-70.41	347.01	-2485.001852	-2484.284795	-2484.235586	-2484.374735	4.47	4.21	3.71	5.27
C3 GS ₁	-121.28	121.21	-2255.973714	-2255.321410	-2255.276831	-2255.406096	0.00	0.00	0.00	0.00
TS ₁	-121.24	214.87	-2255.963342	-2255.311860	-2255.267906	-2255.396296	6.50	5.99	5.69	6.15
GS ₂	-119.54	289.28	-2255.972864	-2255.320652	-2255.276018	-2255.404949	0.53	0.48	0.52	0.72
TS ₂	-121.64	353.48	-2255.965306	-2255.313594	-2255.269723	-2255.396658	5.27	4.90	4.53	5.92

Table 2- CHELPG charges calculated with B3LYP/6-31G* basis-set

Molecule	CHELPG Charges			
	=O	-OH	O32	O33
Curcumin	-0.595*	-0.579*		
A1	-0.584	-0.572	-0.553	-0.544
A2	-0.594	-0.576		
A3	-0.597	-0.569		
C1	-0.591	-0.571	-0.532	-0.534
	-0.646 (w)	-0.600 (w)	-0.572 (w)	-0.573 (w)
	-0.591 (m)	-0.571 (m)	-0.533 (m)	-0.534 (m)
	-0.623 (a)	-0.587(a)	-0.554 (a)	-0.556 (a)
	-0.623 (d)	-0.587 (d)	-0.555 (d)	-0.556 (d)
C2	-0.600	-0.580		
	-0.641 (w)	-0.595 (w)		
	-0.639 (m)	-0.594 (m)		
	-0.620 (a)	-0.584 (a)		
	-0.620 (d)	-0.584 (d)		
C3	-0.601	-0.582		
	-0.654 (w)	-0.608 (w)		
	-0.601 (m)	-0.582 (m)		
	-0.632 (a)	-0.596 (a)		
	-0.632 (d)	-0.598 (d)		

*Values taken from Ref 15. Values calculated in *vacuum* if not specified, (w) water, (m) MeOH, (a) ACN, (d) DMSO.

Table 3- Calculated averaged GIAO magnetic isotropic shielding tensors ($\bar{\sigma}_{\text{calc}}$) for **C1**, **C2** and **C3** in *vacuum* (v), MeOH (m) and DMSO (d).

¹³ C	C1			C2			C3		
	v	m	d	v	m	d	v	m	d
1	88.34	87.94	88.01	88.5	88.19	88.29	88.75	88.64	88.62
2	17.99	17.36	17.65	18.13	17.46	17.77	18.14	17.54	17.82
3	72.92	72.8	72.91	73.34	73.18	73.37	74.28	74.47	74.47
4	54.21	53.84	54.01	54.69	54	54.2	55.27	54.56	54.82
5	62.48	63.47	63.29	64.33	64.36	64.45	66.69	67.35	67.23
6	73.19	73.98	73.96	79.16	77.99	78.37	60.88	60.51	60.69
7	45.32	46.03	45.79	44.92	44.85	44.83	76.35	76.59	76.57
8	49.42	48.2	48.58	48.22	48.5	48.41	36.48	35.8	36.03
9	71.79	71.02	70.95	68.91	69.3	69.1	78.25	77.66	77.72
10	81.35	79.7	80.11	78.51	77.95	78.11	70.32	69.18	69.41
11	84.48	85.92	85.26	89.05	89.5	89.35	86.84	87.8	87.33
12	115.66	116.23	115.72	115.9	116.54	115.88	116.26	116.88	116.26
13	114.94	115.9	115.4	113.79	114.9	114.23	114.3	115.37	114.81
14	119.61	120.01	119.61	119.83	120.26	119.81	120.2	120.63	120.2
15	114.05	115.18	114.52	114.92	116.03	115.35	113.73	114.89	114.26
16	126.04	126.7	126.47	126.08	126.87	126.56	125.87	126.58	126.31
¹ H									
1	27.27	26.76	26.96	27.22	26.74	26.94	27.28	26.79	26.99
3	26.05	25.64	25.82	26.02	25.63	25.82	26.08	25.7	25.86
4	24.85	24.85	24.9	24.87	24.8	24.86	24.85	24.83	24.89
6	25.57	25.42	25.57	25.89	25.52	25.7	25.1	24.89	25.01
7	/	/	/	/	/	/	25.16	25.06	25.13
9	25.19	24.91	25.03	25.16	25.01	25.12	25.34	25.06	25.18
10	25.22	24.89	25.01	24.97	24.72	24.83	24.61	24.32	24.43
11	27.82	26.98	27.53	26.89	26.73	26.86	27.36	26.69	27.15
12	28.49	28.23	28.47	28.43	28.21	28.47	28.39	28.18	28.42
13	28.6	28.19	28.44	28.7	28.28	28.57	28.6	28.17	28.43
14	28.2	28.03	28.22	28.21	28.04	28.25	28.2	28.04	28.24
15	28.94	28.37	28.69	29.09	28.53	28.88	28.87	28.27	28.6
16	28	27.86	27.9	28.16	28	28.06	28.01	27.85	27.9
16	28.14	28.12	28.14	28.41	28.39	28.42	28.22	28.2	28.23

Table 4-Experimental (δ_{exp}) and predicted ($\delta_{\text{pred}} = a \cdot \bar{\sigma}_{\text{calc}} + b$) ^{13}C chemical shifts (ppm) for **C1**, **C2** and **C3** in *vacuum* (v), MeOH (m) and DMSO (d).

	C1						C2						C3					
	δ_{exp} (m)	δ_{pred} (v)	δ_{pred} (m)	δ_{exp} (d)	δ_{pred} (v)	δ_{pred} (d)	δ_{exp} (m)	δ_{pred} (v)	δ_{pred} (m)	δ_{exp} (d)	δ_{pred} (v)	δ_{pred} (d)	δ_{exp} (m)	δ_{pred} (v)	δ_{pred} (m)	δ_{exp} (d)	δ_{pred} (d)	δ_{exp} (m)
1	102.80	101.85	102.50	101.71	103.19	103.62	102.80	102.08	102.56	101.32	103.50	103.76	102.8	102.4	102.8	101.74	103.82	104.01
2	185.40	184.41	184.20	183.50	180.20	180.27	185.60	184.88	184.43	183.68	180.57	180.57	185.6	186.8	186.1	183.57	181.87	181.69
3	124.50	119.95	120.04	122.77	120.07	120.07	124.50	119.92	119.89	122.89	120.11	120.01	124.5	119.7	119.5	122.81	119.81	119.54
4	142.10	141.90	141.98	140.56	140.55	140.66	142.10	141.86	142.12	140.69	140.53	140.89	142.1	142.4	142.6	140.31	140.82	141.10
5	132.60	132.20	131.22	129.54	131.50	130.55	132.10	130.52	130.25	128.91	129.97	129.73	131.6	128.8	128.0	128.78	128.20	127.48
6	116.20	119.63	118.83	121.45	119.78	118.92	112.10	113.07	114.07	111.60	113.73	114.57	131.6	135.7	135.7	130.32	134.62	134.66
7	147.70	152.34	151.53	147.27	150.28	149.61	149.60	153.36	152.99	149.47	151.23	151.10	118.9	117.2	117.0	116.94	117.52	117.24
8	149.40	147.53	148.29	147.53	145.80	146.57	150.10	149.47	148.84	148.85	147.61	147.20	161.6	164.9	164.7	159.5	161.60	161.71
9	118.80	121.27	122.31	116.31	121.31	122.20	117.30	125.13	124.83	115.42	124.96	124.67	118.9	115.0	115.7	116.94	115.42	115.97
10	122.80	110.06	111.67	114.98	110.84	112.22	122.50	113.84	114.37	122.83	114.44	114.85	131.6	124.4	125.4	130.32	124.19	125.09
11	96.30	106.38	105.70	101.58	107.42	106.61	99.40	101.43	101.32	99.97	102.90	102.61	96.5	104.7	104.4	100.34	105.93	105.43
12	68.10	69.79	70.34	76.96	73.28	73.43	68.10	69.84	70.52	73.52	73.50	73.71	68.4	69.5	70.3	73.55	73.41	73.69
13	71.40	70.64	70.73	69.92	74.07	73.78	70.50	72.32	72.44	77.23	75.81	75.51	71.2	71.9	72.1	76.98	75.57	75.28
14	65.00	65.16	65.81	73.42	68.96	69.19	66.20	65.22	65.95	69.97	69.19	69.43	66.7	64.8	65.7	70.06	69.05	69.37
15	70.10	71.68	71.74	75.93	75.05	74.74	69.70	71.00	71.14	77.51	74.57	74.29	68.7	72.6	72.7	77.52	76.20	75.89
16	59.20	57.61	57.86	60.80	61.92	61.72	59.20	57.86	58.12	61.14	62.35	62.08	58.3	58.0	58.5	61.07	62.78	62.67
a		-1.174	-1.161		-1.095	-1.089		-1.177	-1.161		-1.095	-1.089		-1.195	-1.176		-1.105	-1.097
b		205.52	204.69		199.90	199.50		206.21	205.06		200.42	199.93		208.51	207.09		201.92	201.24
R ²		0.9834	0.9878		0.9905	0.9915		0.9906	0.9917		0.9879	0.9882		0.9896	0.9911		0.9933	0.9939

Table 5- Experimental (δ_{exp}) and predicted ($\delta_{\text{pred}} = a \cdot \bar{\sigma}_{\text{calc}} + b$) ^1H chemical shifts (ppm) for **C1**, **C2** and **C3** in *vacuum* (v). MeOH (m) and DMSO (d).

^1H	C1						C2						C3					
	δ_{exp} (m)	δ_{pred} (v)	δ_{pred} (m)	δ_{exp} (d)	δ_{pred} (v)	δ_{pred} (d)	δ_{exp} (m)	δ_{pred} (v)	δ_{pred} (m)	δ_{exp} (d)	δ_{pred} (v)	δ_{pred} (d)	δ_{exp} (m)	δ_{pred} (v)	δ_{pred} (m)	δ_{exp} (d)	δ_{pred} (d)	δ_{pred} (m)
1	6.01	5.05	5.27	6.12	4.96	5.17	6.02	5.07	5.31	6.13	5.03	5.25	6.01	4.98	4.97	6.11	4.89	5.09
3	6.63	6.40	6.58	6.75	6.39	6.54	6.72	6.38	6.56	6.87	6.44	6.57	6.69	6.31	6.26	6.83	6.31	6.44
4	7.53	7.74	7.50	7.52	7.80	7.64	7.6	7.63	7.50	7.6	7.79	7.71	7.62	7.67	7.40	7.61	7.76	7.60
6	7.14	6.94	6.83	7.13	6.96	6.84	7.12	6.52	6.69	7.38	6.59	6.71	7.14	7.40	7.25	7.7	7.46	7.46
7	/	/	/	/	/	/	/	/	/	/	/	/	7.61	7.33	7.11	7.09	7.39	7.32
9	7.20	7.36	7.43	7.13	7.40	7.48	7.18	7.31	7.26	7.13	7.45	7.40	7.60	7.13	7.05	7.09	7.18	7.26
10	7.07	7.32	7.45	7.2	7.37	7.51	7.18	7.52	7.59	7.26	7.67	7.74	7.14	7.94	7.92	7.7	8.04	8.15
11	4.97	4.44	5.01	4.81	4.31	4.49	4.98	5.43	5.32	4.99	5.42	5.34	4.98	4.90	4.79	4.96	4.79	4.90
12	3.53	3.69	3.55	3.30	3.52	3.37	3.53	3.75	3.65	3.27	3.61	3.44	3.52	3.76	3.33	3.27	3.58	3.38
13	3.47	3.57	3.60	3.18	3.40	3.40	3.48	3.45	3.57	3.28	3.29	3.32	3.47	3.52	3.30	3.29	3.33	3.37
14	3.44	4.02	3.79	3.32	3.87	3.67	3.43	3.99	3.84	3.17	3.87	3.70	3.42	3.97	3.55	3.17	3.80	3.60
15	3.45	3.19	3.39	3.36	3.00	3.10	3.45	3.03	3.28	3.34	2.83	2.95	3.45	3.22	3.11	3.37	3.01	3.17
16	3.90	4.24	3.98	3.72	4.10	4.05	3.89	4.04	3.88	3.67	3.93	3.92	3.91	4.18	3.93	3.69	4.03	4.00
16'	3.71	4.08	3.68	3.48	3.94	3.76	3.71	3.77	3.44	3.45	3.63	3.50	3.71	3.94	3.55	3.46	3.78	3.61
a		-1.110	-1.168		-1.175	-1.197		-1.091	-1.131		-1.175	-1.183		-1.107	-1.150		-1.181	-1.196
b		35.324	36.527		37.003	37.442		34.772	35.537		37.019	37.1198		35.183	36.005		37.103	37.359
R ²		0.9399	0.9718		0.9295	0.9553		0.9232	0.9524		0.9186	0.9465		0.9362	0.9479		0.9399	0.9611

1
2
3
4
5
6
7
8
9
10
11
12
13
14
15
16
17
18
19
20
21
22
23
24
25
26
27
28
29
30
31
32
33
34
35
36
37
38
39
40
41
42
43
44
45
46
47
48
49
50
51
52
53
54
55
56
57
58
59
60**Table 6-** Uv-vis band maximum position (nm) in different solvents for **C1** compound.

	Vacuum	H ₂ O		MeOH		ACN		DMSO	
	calc	exp	calc	exp	calc	exp	calc	exp	calc
C1	402	414	423	411	422	405	419	423	421
C2	413	413	432	411	432	413	428	425	431
C3	403	408	425	406	425	405	420	416	423

For Peer Review

Caption of Figures

Figure 1: General structure of the studied curcumin glucosyl derivatives.

Figure 2: ΔG for compounds **A1**, **A2** and **A3** as function of the rotational dihedral angle ϕ .

Figure 3: Final optimized structures of **A** compounds at B3LYP/6-31G* level at GS₁ and GS₂ state. The hydrogen interaction is represented by dots.

Figure 4: Top view of **C2** optimized structures at B3LYP/6-31G* level showing the different sugar spatial positions with respect to curcumin planar skeleton and their total energies (a.u.).

Figure 5: Representation of HOMO and LUMO orbital density for **A** and **C** series at B3LYP/6-31G* level.

Figure 6: Molecular electrostatic maps in *vacuum* of **A** and **C** compounds in their GS₁ state at B3LYP/6-31G* level.

Figure 7: ¹H NMR spectrum of **C1** in DMSO-*d*₆ (* residual DMSO)

Figure 8: Plots of DMSO-*d*₆ vs. MeOD experimental ¹H (**A**) and ¹³C (**B**) chemical shifts (δ) for glucosyl-curcuminoids: **C1** (∇), **C2** (\square) and **C3** (\circ).

Figure 9: Plot of ¹H and ¹³C δ_{exp} vs. $\bar{\sigma}_{\text{calc}}$ for **C1**. Solid circle is referred to H-1 proton, dotted circle highlights anomeric proton (H-11).

Figure 10: Correlation between experimental and B3LYP/6-311G* in *vacuum* calculated wavenumbers for **C1**. Equation: $\bar{\nu}_{\text{exp}} = a \cdot \bar{\nu}_{\text{calc}}$; $a = 0.9991$, $R^2 = 0.9983$.

Figure 1

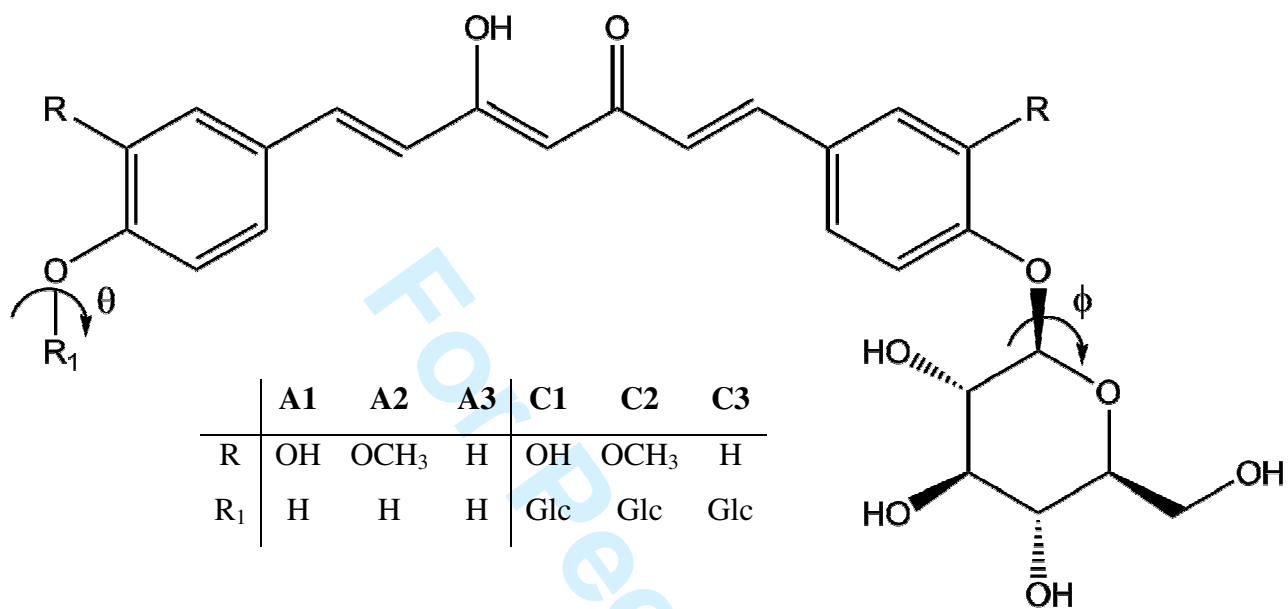


Figure 2

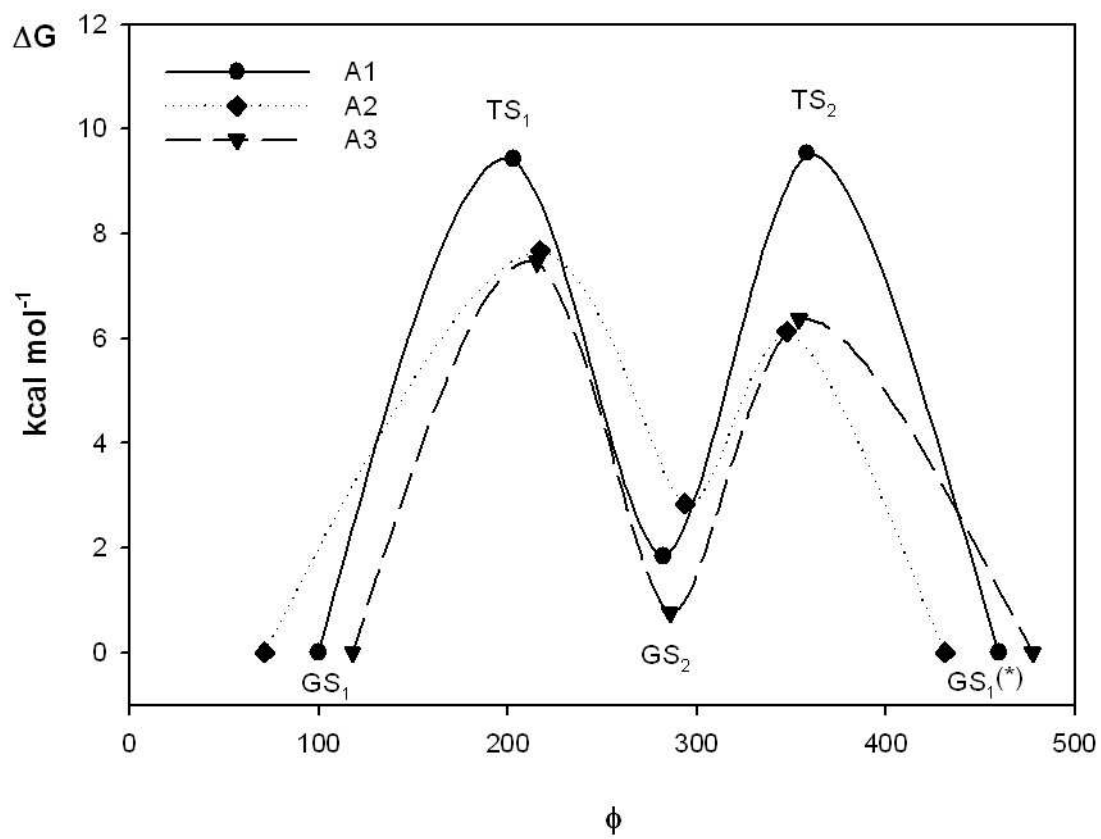


Figure 3

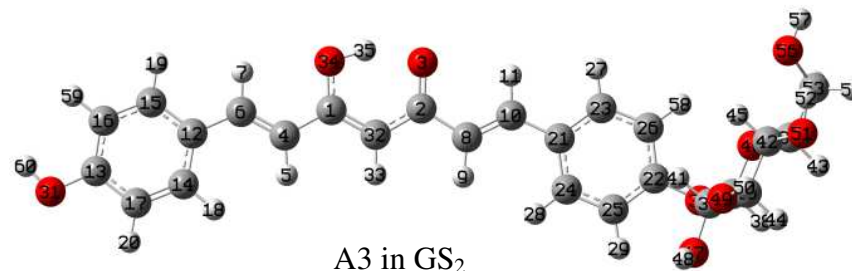
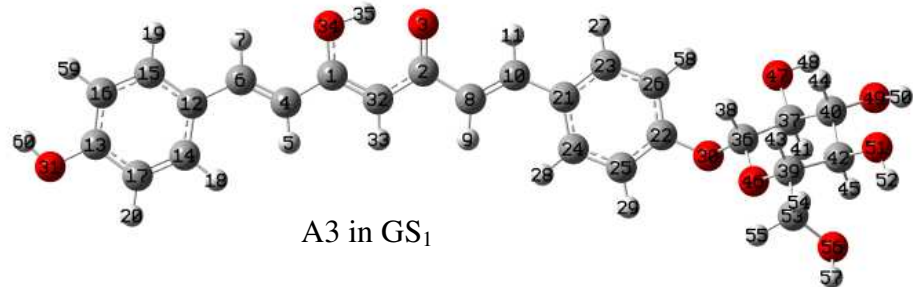
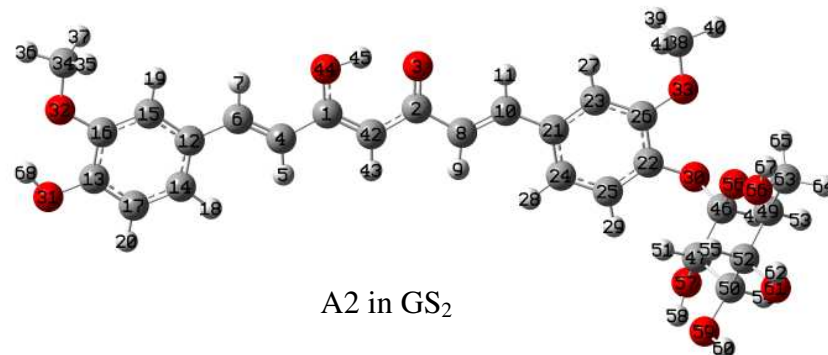
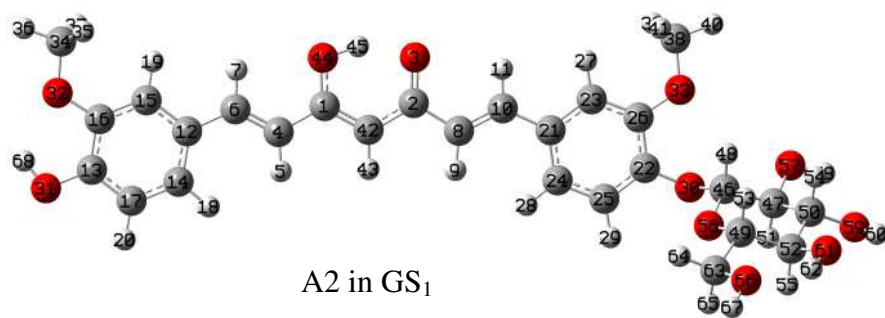
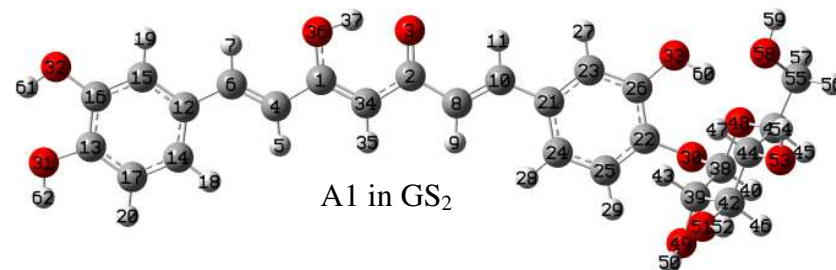
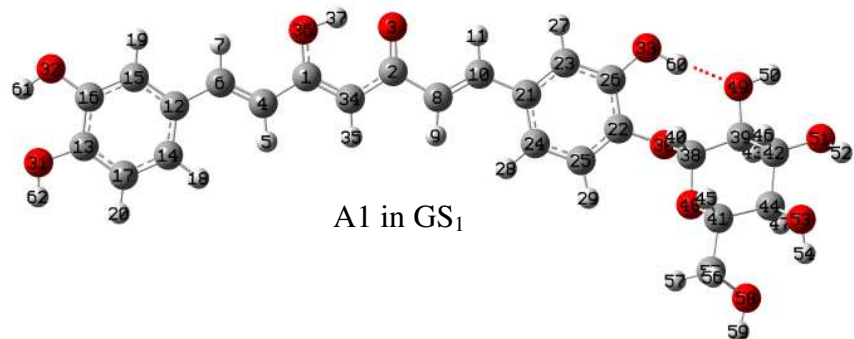
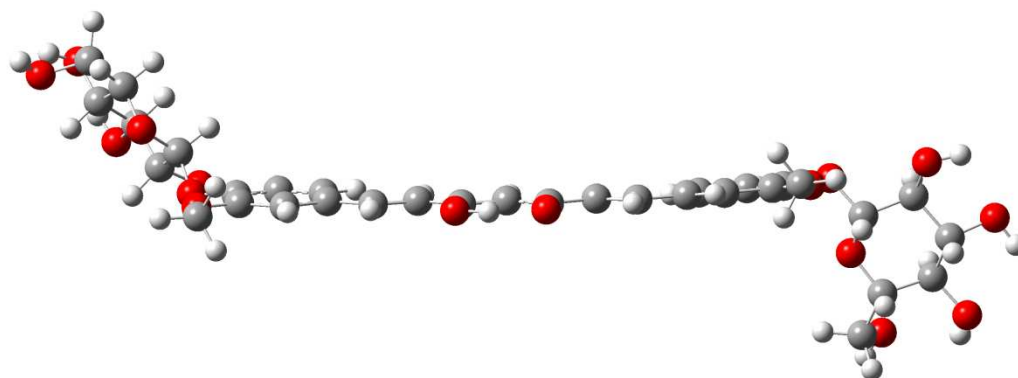
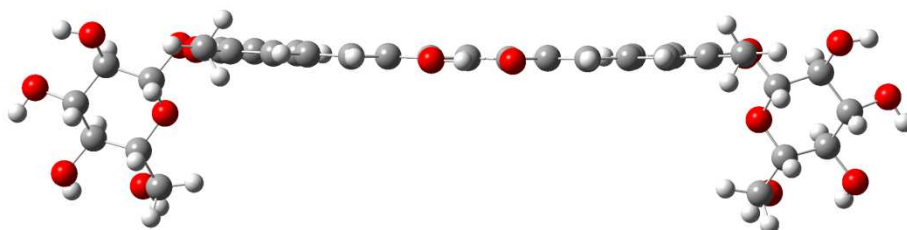


Figure 4



sin-anti configuration $E = -2485.008088$ a.u.



sin-sin configuraton $E = -2485.008984$ a.u.

Figure 5

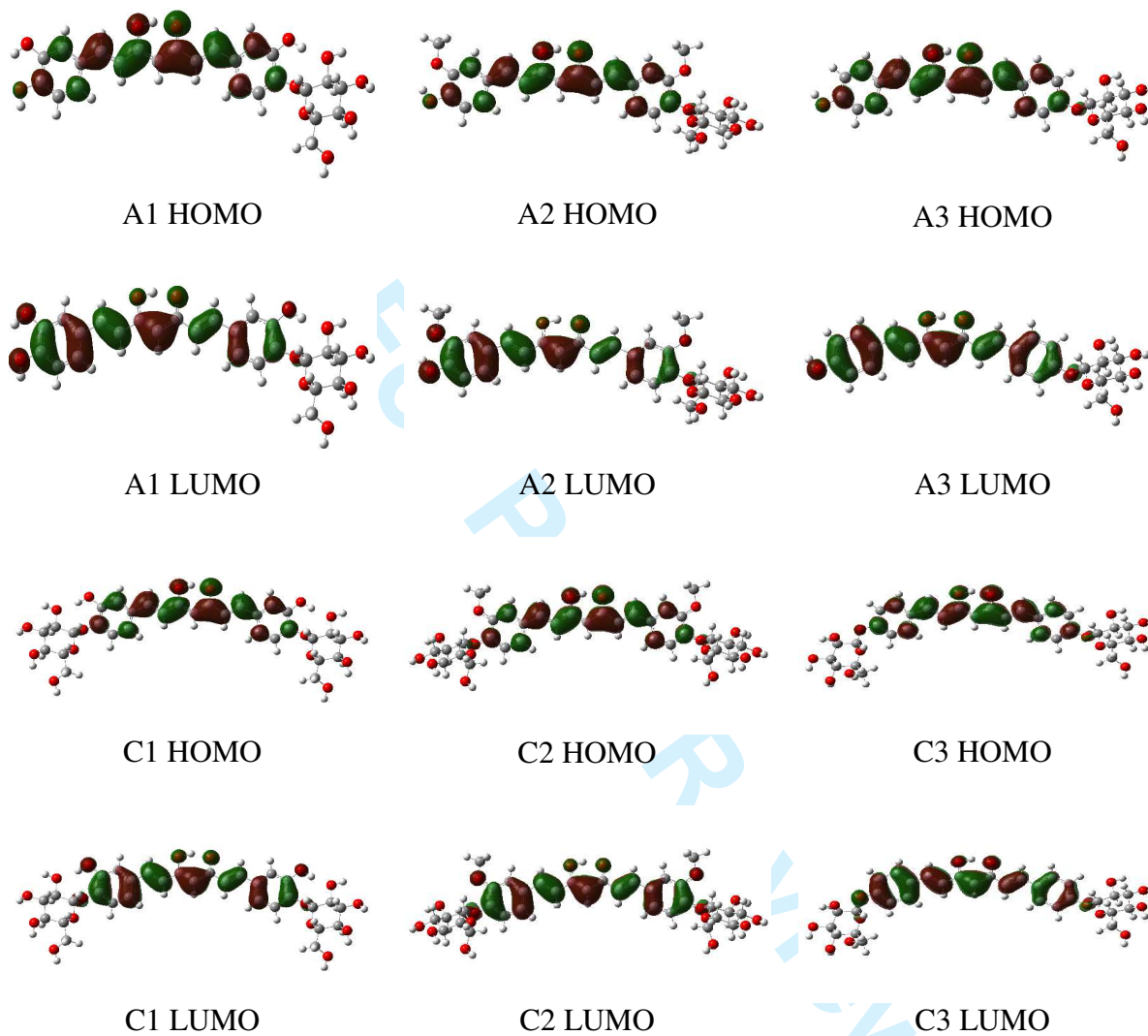


Figure 6

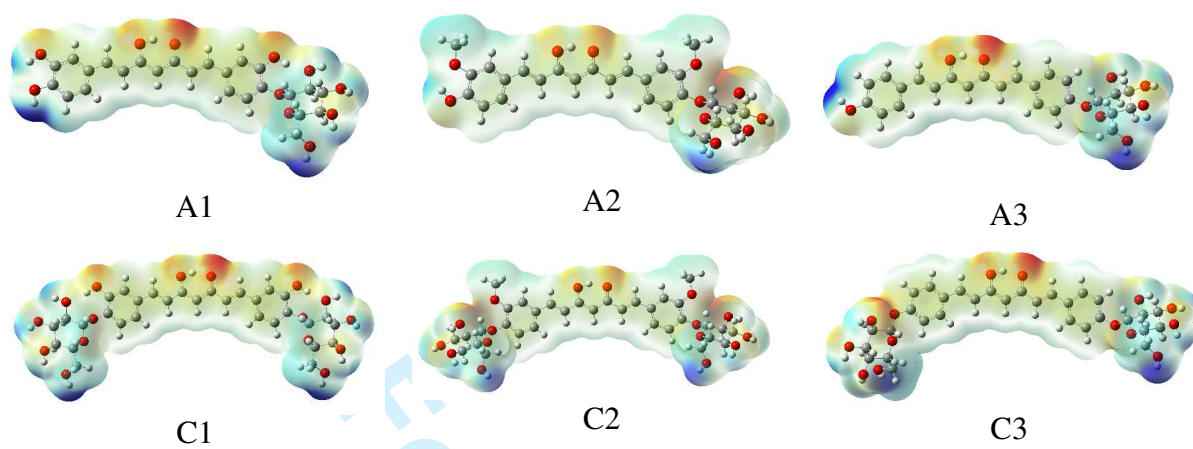


Figure 7

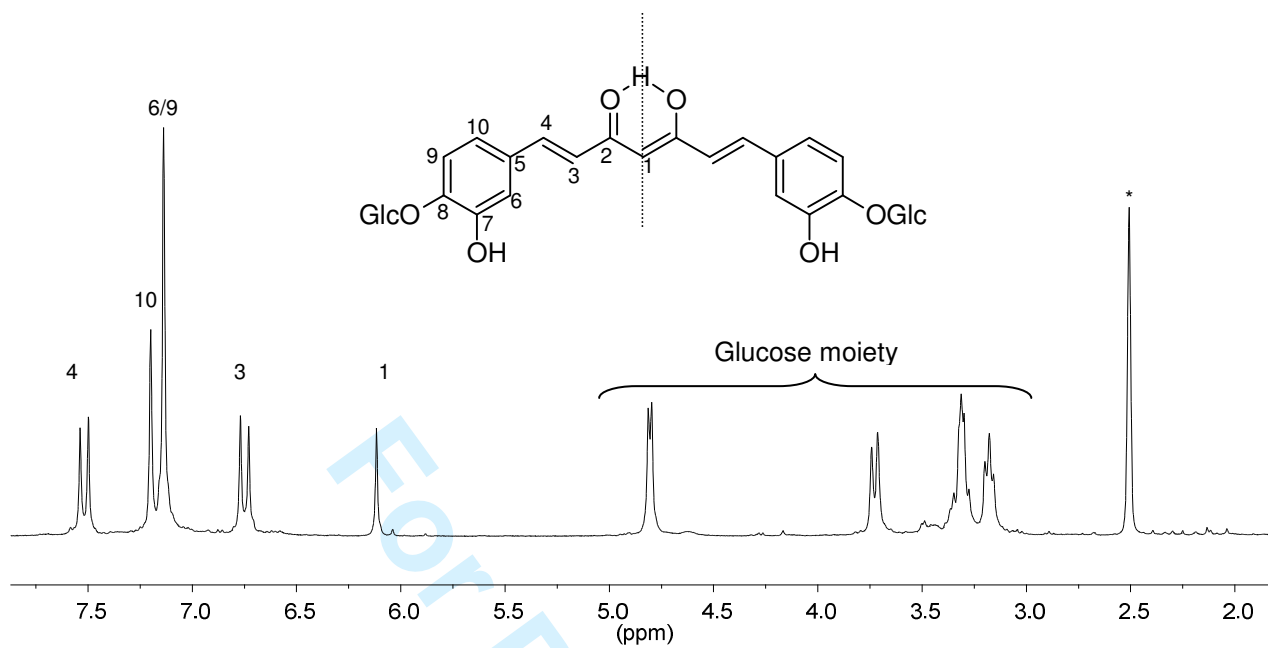


Figure 8

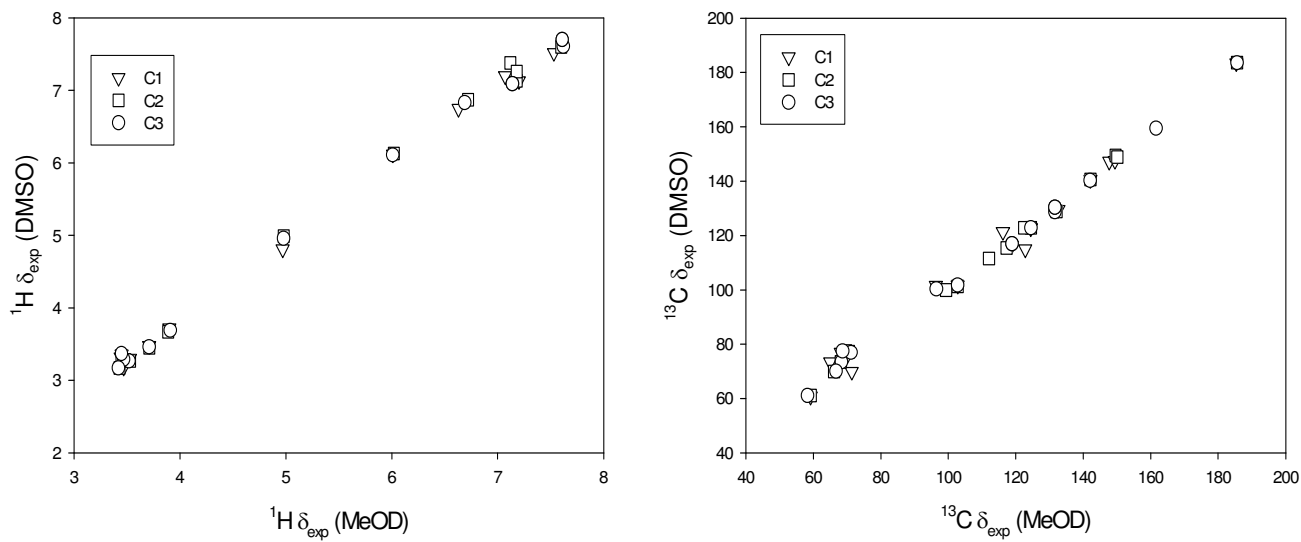


Figure 9

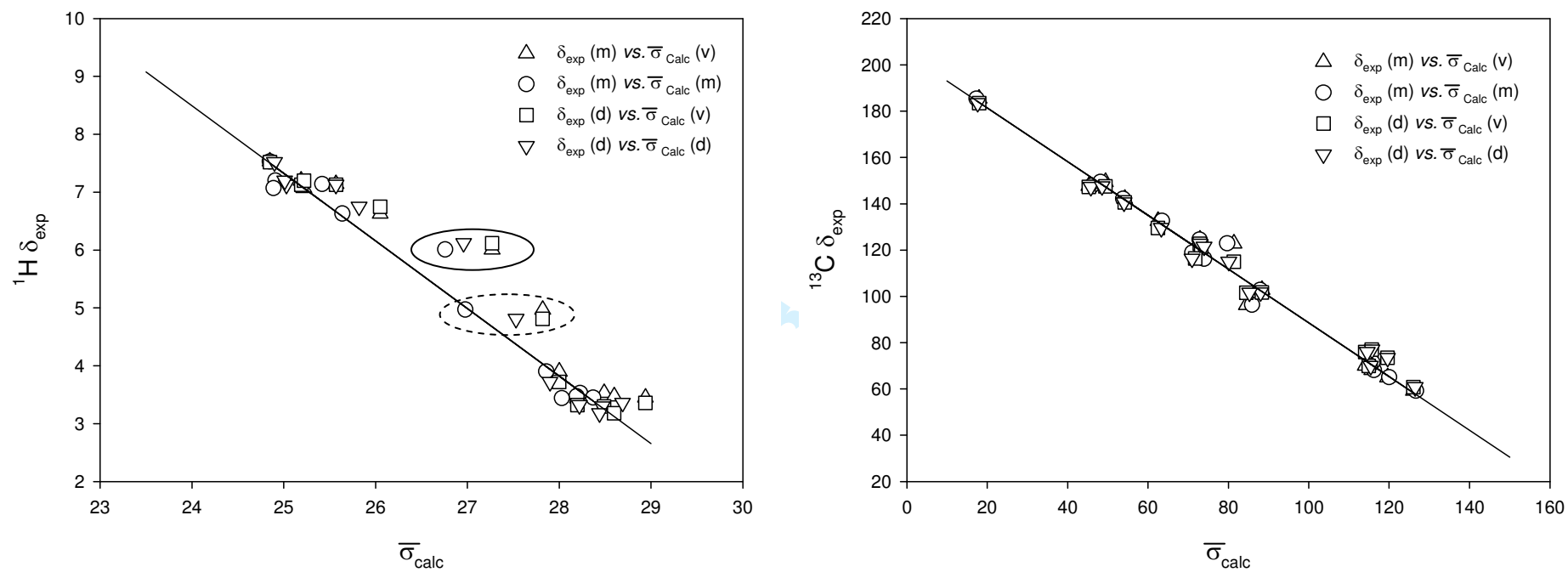
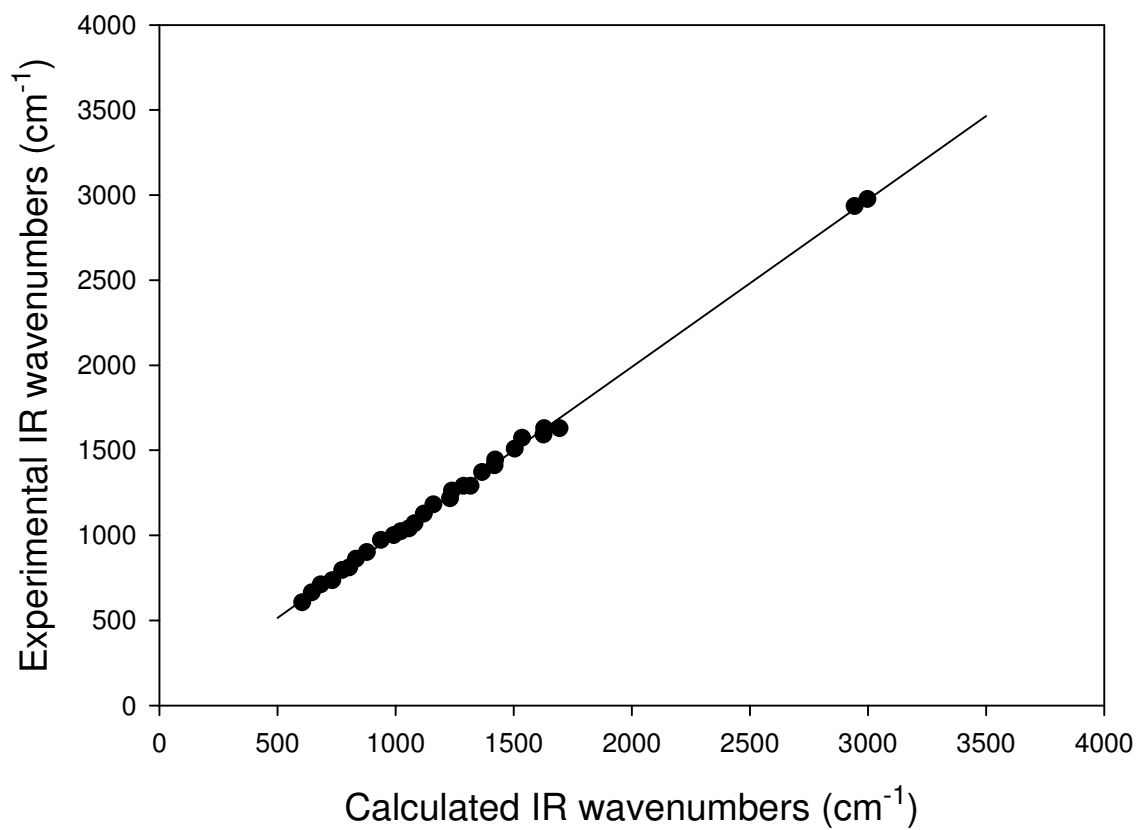
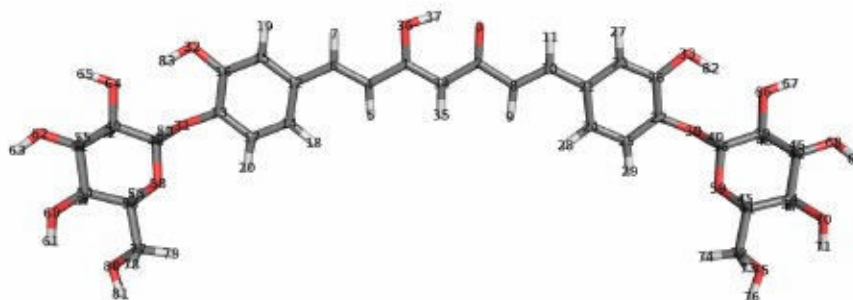


Figure 10



Review

Table 1: NMR values for C1 compound calculated in *vacuum*, H₂O, MeOH, ACN and DMSO.

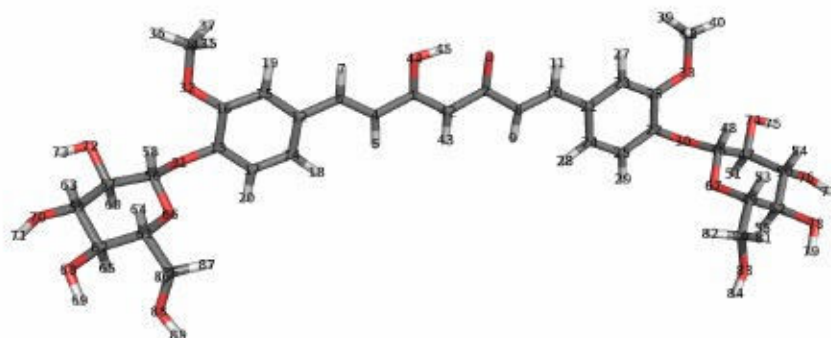
ATOM N	<i>vacuum</i>	H ₂ O	MeOH	ACN	DMSO
1	25.37	24.94	24.95	25.17	25.17
2	10.62	9.72	9.77	10.15	10.15
4	74.48	74.58	74.63	74.69	74.69
5	26.18	25.74	25.77	25.95	25.95
6	55.32	54.75	54.74	54.92	54.93
7	24.95	24.92	24.92	24.98	24.98
8	71.37	70.91	70.98	71.14	71.14
9	25.93	25.49	25.52	25.7	25.7
10	53.11	52.98	52.95	53.11	53.11
11	24.75	24.79	24.79	24.84	24.84
12	62.48	63.4	63.38	63.23	63.23
13	49.51	48.29	48.32	48.69	48.68
14	81.55	79.78	79.87	80.3	80.28
15	73.57	74.35	74.3	74.26	74.27
16	45.3	46.06	46.03	45.78	45.78
17	71.73	71.01	70.99	70.94	70.92
18	25.26	24.9	24.92	25.05	25.05
19	25.62	25.45	25.46	25.61	25.61
20	25.19	24.92	24.92	25.04	25.03
21	62.49	63.59	63.56	63.34	63.35
22	49.34	48.06	48.09	48.49	48.49
23	72.82	73.72	73.67	73.64	73.65
24	81.16	79.45	79.54	79.95	79.94
25	71.86	71.06	71.05	71	70.99
26	45.36	46.07	46.04	45.8	45.81
27	25.53	25.38	25.39	25.54	25.54
28	25.19	24.84	24.86	24.99	24.99
29	25.19	24.91	24.92	25.03	25.03
34	88.34	87.9	87.95	88.02	88.02
35	27.27	26.73	26.76	26.97	26.97
36	189.29	193.45	193.26	192.29	192.32
37	18.36	18.58	18.57	18.54	18.54
38	84.49	86.03	85.93	85.26	85.27
39	115.67	116.25	116.24	115.72	115.72
40	27.82	26.92	26.98	27.54	27.53
41	114.06	115.26	115.18	114.51	114.52
42	114.93	115.95	115.9	115.38	115.39
43	28.5	28.23	28.23	28.47	28.47
44	119.61	120.01	120.01	119.62	119.62
45	28.94	28.34	28.38	28.7	28.69
46	28.6	28.17	28.19	28.45	28.45
47	28.2	28.04	28.04	28.23	28.23
48	84.47	86.02	85.92	85.26	85.26
49	115.67	116.25	116.24	115.72	115.72
50	27.83	26.92	26.99	27.54	27.54

Continued on next page

Table 1 – continued from previous page

ATOM N.	<i>vacuum</i>	H ₂ O	MeOH	ACN	DMSO
51	114.95	115.96	115.91	115.39	115.41
52	28.5	28.24	28.24	28.47	28.48
53	114.05	115.25	115.18	114.51	114.52
54	119.63	120.02	120.02	119.63	119.62
55	28.6	28.17	28.2	28.45	28.45
56	28.95	28.35	28.38	28.7	28.7
57	28.21	28.04	28.04	28.23	28.23
61	30.54	29.9	29.91	30.21	30.21
63	30.08	29.55	29.56	29.87	29.87
65	29.99	29.25	29.29	29.68	29.68
67	29.99	29.25	29.29	29.67	29.67
69	30.08	29.55	29.56	29.87	29.87
71	30.54	29.9	29.91	30.21	30.21
72	126.03	126.73	126.7	126.47	126.47
73	28	27.85	27.86	27.91	27.91
74	28.15	28.13	28.13	28.15	28.15
76	32.03	30.77	30.81	31.33	31.32
77	126.05	126.74	126.71	126.48	126.48
78	28.01	27.86	27.86	27.91	27.91
79	28.15	28.13	28.13	28.15	28.15
81	32.03	30.78	30.82	31.33	31.32
82	25.17	25.02	25.03	25.07	25.07
83	25.16	25.02	25.03	25.07	25.07

Table 2: NMR values for C2 compound calculated in *vacuum*, H₂O, MeOH, ACN and DMSO. Oxygen atom chemical shifts are omitted.



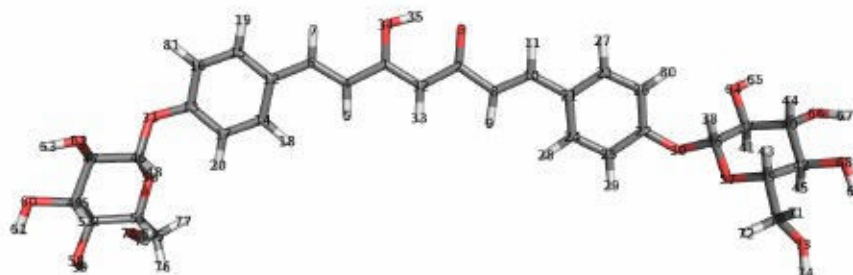
ATOM N	<i>vacuum</i>	H ₂ O	MeOH	ACN	DMSO
1	25.5	24.99	25.01	25.24	25.24
2	10.76	9.88	9.93	10.32	10.32
4	74.94	74.98	75.02	75.17	75.17
5	26.15	25.74	25.76	25.95	25.95
6	55.83	54.9	54.91	55.13	55.13
7	24.98	24.86	24.87	24.94	24.94
8	71.75	71.28	71.34	71.57	71.58
9	25.9	25.49	25.51	25.69	25.69
10	53.57	53.11	53.09	53.3	53.28
11	24.77	24.73	24.73	24.79	24.78
12	64.32	64.26	64.26	64.37	64.38
13	48.31	48.6	48.63	48.52	48.52
14	78.72	78.04	78.12	78.28	78.28
15	79.53	78.2	78.3	78.68	78.68
16	44.9	44.85	44.86	44.84	44.83
17	68.85	69.41	69.26	69.07	69.06
18	25.01	24.73	24.75	24.87	24.87
19	25.95	25.53	25.56	25.74	25.74
20	25.16	25.02	25.02	25.13	25.13
21	64.34	64.46	64.46	64.51	64.52
22	48.14	48.37	48.39	48.33	48.32
23	78.8	77.59	77.68	78.08	78.07
24	78.32	77.7	77.79	77.94	77.94
25	68.99	69.48	69.34	69.15	69.14
26	44.95	44.86	44.86	44.86	44.85
27	25.85	25.45	25.48	25.67	25.67
28	24.94	24.68	24.7	24.81	24.81
29	25.17	25.01	25.01	25.13	25.13
34	137.41	137.57	137.56	137.34	137.34
35	28.57	28.35	28.36	28.43	28.43
36	28.14	28.06	28.06	28.1	28.1
37	28.65	28.51	28.52	28.59	28.59
38	137.39	137.55	137.53	137.32	137.32
39	28.63	28.5	28.5	28.57	28.57
40	28.14	28.05	28.05	28.09	28.09
41	28.55	28.33	28.35	28.42	28.42
42	88.51	88.15	88.2	88.3	88.3
43	27.23	26.71	26.74	26.95	26.95
45	18.33	18.52	18.51	18.49	18.49
46	89.08	89.77	89.52	89.37	89.37
47	115.9	116.53	116.54	115.88	115.88
48	26.89	26.47	26.72	26.85	26.86
49	114.93	116.16	116.04	115.36	115.36
50	113.79	114.93	114.89	114.23	114.23

Continued on next page

Table 2 – continued from previous page

ATOM N.	<i>vacuum</i>	H ₂ O	MeOH	ACN	DMSO
51	28.43	28.23	28.21	28.47	28.48
52	119.82	120.21	120.26	119.82	119.81
53	29.09	28.5	28.54	28.89	28.89
54	28.7	28.26	28.28	28.57	28.57
55	28.22	28.07	28.04	28.24	28.25
56	89.04	89.75	89.49	89.35	89.34
57	115.91	116.54	116.56	115.89	115.89
58	26.91	26.48	26.74	26.87	26.87
59	113.8	114.94	114.91	114.24	114.24
60	28.43	28.23	28.21	28.48	28.48
61	114.92	116.15	116.04	115.35	115.35
62	119.84	120.23	120.28	119.84	119.82
63	28.7	28.27	28.28	28.58	28.58
64	29.09	28.5	28.54	28.89	28.89
65	28.22	28.07	28.04	28.24	28.25
69	30.67	30.02	30.02	30.31	30.31
71	30.18	29.59	29.63	29.93	29.93
73	30.5	29.88	29.96	30.29	30.29
75	30.5	29.88	29.95	30.28	30.29
77	30.18	29.59	29.63	29.93	29.93
79	30.67	30.01	30.02	30.31	30.3
80	126.08	126.89	126.88	126.57	126.57
81	28.17	28	28	28.06	28.06
82	28.41	28.4	28.4	28.42	28.42
84	32.17	30.85	30.89	31.42	31.41
85	126.09	126.9	126.88	126.57	126.57
86	28.17	28	28.01	28.06	28.06
87	28.42	28.4	28.4	28.42	28.42
89	32.17	30.85	30.89	31.42	31.41

Table 3: NMR values for C3 compound calculated in *vacuum*, H₂O, MeOH, ACN and DMSO. Oxygen atom chemical shifts are omitted.



ATOM N	<i>Vacuum</i>	H ₂ O	MeOH	ACN	DMSO
1	25.43	24.95	24.97	25.18	25.18
2	10.86	10.08	10.13	10.47	10.47
4	76.13	76.66	76.7	76.58	76.58
5	26.24	25.82	25.85	26.02	26.01
6	56.42	55.38	55.38	55.71	55.71
7	24.97	24.91	24.91	24.98	24.98
8	72.44	72.2	72.25	72.36	72.36
9	25.94	25.52	25.55	25.72	25.72
10	54.12	53.76	53.74	53.96	53.95
11	24.74	24.76	24.76	24.8	24.8
12	67.23	67.9	67.89	67.74	67.74
13	37.49	36.71	36.72	37.03	37.02
14	70.18	68.76	68.85	69.07	69.05
15	61.48	61.18	61.15	61.35	61.35
16	77.04	77.78	77.69	77.6	77.61
17	81.5	80.29	80.39	80.56	80.55
18	24.65	24.32	24.34	24.45	24.45
19	25.14	24.94	24.94	25.06	25.06
20	25.39	25.01	25.05	25.16	25.16
21	66.15	66.86	66.83	66.71	66.72
22	35.48	34.87	34.88	35.07	35.06
23	60.28	59.88	59.89	60.04	60.05
24	70.47	69.46	69.51	69.78	69.77
25	75.01	74.96	74.94	74.9	74.89
26	75.66	75.48	75.51	75.53	75.53
27	25.06	24.85	24.85	24.97	24.97
28	24.58	24.29	24.31	24.42	24.42
29	25.3	25.07	25.08	25.21	25.2
32	88.76	88.6	88.64	88.63	88.63
33	27.28	26.77	26.8	27	26.99
35	18.33	18.56	18.55	18.52	18.52
36	84.51	85.52	85.42	84.97	84.97
37	115.85	116.52	116.52	115.88	115.87
38	27.37	26.68	26.76	27.17	27.17
39	113.59	114.88	114.8	114.13	114.13
40	114.15	115.28	115.25	114.66	114.67
41	28.45	28.23	28.23	28.47	28.47
42	119.84	120.29	120.28	119.85	119.84
43	28.94	28.33	28.36	28.7	28.7
44	28.55	28.1	28.12	28.39	28.39
45	28.24	28.07	28.07	28.27	28.27
46	89.18	90.29	90.19	89.71	89.71
47	116.67	117.26	117.26	116.65	116.65
48	27.37	26.53	26.63	27.14	27.14

Continued on next page

Table 3 – continued from previous page

<u>ATOM N</u>	<u>VACUO</u>	<u>H₂O</u>	<u>MeOH</u>	<u>ACN</u>	<u>DMSO</u>
49	114.46	115.58	115.51	114.96	114.97
50	28.34	28.14	28.14	28.37	28.37
51	113.87	115.07	114.99	114.38	114.4
52	120.56	120.93	120.99	120.58	120.57
53	28.65	28.21	28.23	28.5	28.49
54	28.8	28.16	28.2	28.53	28.52
55	28.18	28.05	28.02	28.21	28.21
59	30.52	29.9	29.85	30.2	30.2
61	30.06	29.48	29.53	29.82	29.82
63	30.44	29.85	29.89	30.23	30.24
65	30.26	29.66	29.72	30.03	30.04
67	30.11	29.55	29.6	29.88	29.88
69	30.46	29.83	29.87	30.14	30.14
70	125.83	126.59	126.59	126.28	126.29
71	28.05	27.89	27.89	27.94	27.94
72	28.24	28.25	28.24	28.27	28.26
74	32.08	30.79	30.83	31.35	31.35
75	125.92	126.6	126.58	126.33	126.33
76	27.98	27.81	27.82	27.86	27.86
77	28.2	28.17	28.17	28.2	28.2
79	32.05	30.79	30.83	31.34	31.34
80	24.96	24.88	24.89	24.92	24.92
81	25.38	25.24	25.24	25.36	25.36

Table 4: Vibrational modes of C1: ν , stretching; δ , γ in-plane and out-plane bending, respectively; τ , torsion; superscript: Ph, aromatic ring vibrations; A, vibrations connected with 'enolic' part of the molecule(left); B, vibrations connected with 'keto' part of the molecule(right).

ν_{IR}^{EXP}	ν_{IR}^{ASS}	ν_{IR}^{CALC}	ν_{IR}^{CALC}	ν_{IR}^{CALC}	Assignment
		601	23.75	ν^{CC}	γ_{COC}
					$\gamma_{C=CH}$
605	γ_{COH}	605	142.03		γ_{COH}
					$\gamma_{CC=O}$
		622	5.09		γ_{CCC}^{Ph}
		623	23.69	δ_{CCC}	
				δ_{CCC}^{PhB}	
		628	9.09		γ_{CCC}^{PhB}
		644	40.35		τ_{CCOH}
		646	173.64		τ_{CCOH}
663	δ_{CCC}				
	δ_{CCC}^{Ph}				
	γ_{CCC}				
	γ_{CCC}^{Ph}				
		678	1.19	$\delta_{CC=C}$	
				δ_{CCC}^{PhA}	
		682	2.06		γ_{CCC}^S
		683	12.31		γ_{CCC}^S
		693	0.42		$\gamma_{C=CH}^{PhB}$
					$\gamma_{C=C-OH}$
					$\gamma_{C=CH}^{PhA}$
711	γ_{CCC}^{Ph}				
		725	2.68		γ_{CCC}^{PhA}
		732	4.65		γ_{CCC}^{PhA}

Continued on next page

Table 4 – continued from previous page

$\nu_{\text{IR}}^{\text{EXP}}$	$\nu_{\text{IR}}^{\text{CALC}}$	$\nu_{\text{IR}}^{\text{CALC}}$	$\text{km} \cdot \text{mol}^{-1}$	Assignment
734	$\gamma_{\text{CCcP h}}$			$\gamma_{\text{CCc}}^{\text{P h}}$
	$\delta_{\text{CCC}}^{\text{P h}}$			
	δ_{CCc}			
	γ_{CCH}			
		747	3.92	$\gamma_{\text{CCc}}^{\text{P hb}}$
				$\gamma_{\text{cK-CH}}$
		754	8.52	$\delta_{\text{CCC}}^{\text{P hA}}$
				$\delta_{\text{CCC}}^{\text{P hB}}$
				$\delta_{\text{CCO}}^{\text{K}}$
		774	11.89	$\gamma_{\text{cK-CH}}$
795	$\gamma_{\text{CCcP h}}$			
		804	66.38	$\gamma_{\text{CCc}}^{\text{P hb}}$
				$\gamma_{\text{CCc}}^{\text{P hA}}$
810	$\gamma_{\text{CCH}}^{\text{P h}}$			
		812	22.66	$\gamma_{\text{CCH}}^{\text{P hB}}$
				$\gamma_{\text{CCH}}^{\text{P hA}}$
		815	1.49	$\gamma_{\text{CCH}}^{\text{P hB}}$
				$\gamma_{\text{CCH}}^{\text{P hA}}$
		829	22.98	$\gamma_{\text{CCH}}^{\text{P hb}}$
				$\gamma_{\text{CCH}}^{\text{P hA}}$
		833	10.35	$\delta_{\text{cc=C}}$
				$\gamma_{\text{CCH}}^{\text{P hA}}$
				$\gamma_{\text{CCH}}^{\text{P hB}}$
		852	3.77	$\delta_{\text{CC=O}}^{\text{K}}$

Continued on next page

Table 4 – continued from previous page

1
2
3
4
5
6
7
8
9
10
11
12
13
14
15
16
17
18
19
20
21
22
23
24
25
26
27
28
29
30
31
32
33
34
35
36
37
38
39
40
41
42
43
44
45
46
47
48
49
50
51
52
53
54
55
56
57
58
59
60

$\nu_{\text{IR}}^{\text{EXP}} / \text{ASS} \nu_{\text{IR}}^{\text{CALC}} / \text{A} / \text{CALC}_{\text{IR}} / \text{km} \cdot \text{mol}^{-1}$			Assignment			
				$\delta_{\text{CCC}}^{\text{K}}$		
				$\delta_{\text{cc}=\text{C}}$		
				$\delta_{\text{CCC}}^{\text{P h}_A}$		
				$\delta_{\text{CCC}}^{\text{P h}_B}$		
862	$\gamma_{\text{CCH}^{\text{P h}}}$	873	4.58		γ_{CCH}	
					$\gamma_{\text{CCH}}^{\text{P h}_B}$	
					$\gamma_{\text{CCH}}^{\text{P h}_A}$	
		878	36.47		$\gamma_{\text{CCH}}^{\text{P h}_B}$	
900	γ_{ccc}	900	0.42		γ_{CCH}	
	δ_{cco}					
	τ_{CCOH}					
		903	1.22		γ_{CCH}	
		909	20.99	$\delta_{\text{CC}_2\text{OH}}^{\text{S}}$	$\gamma_{\text{CCH}}^{\text{S}}$	
		909	2.52	$\delta_{\text{CC}_2\text{OH}}^{\text{S}}$	$\gamma_{\text{CCH}}^{\text{S}}$	
		935	12.41		$\gamma_{\text{CCH}}^{\text{P h}_A}$	$\tau_{\text{CCOH}}^{\text{K}}$
		936	3.52		$\gamma_{\text{CCH}}^{\text{P h}_B}$	
		938	89.84		$\gamma_{\text{CCH}}^{\text{P h}_A}$	$\tau_{\text{CCOH}}^{\text{K}}$
		969	24.33	$\delta_{\text{CC}^{\text{B}}_2\text{OH}}^{\text{S}}$	$\gamma_{\text{CCH}}^{\text{S}_B}$	
		969	18.38	$\delta_{\text{CC}^{\text{A}}_2\text{OH}}^{\text{S}}$	$\gamma_{\text{CCH}}^{\text{S}_A}$	
972	ν_{co}					
	ν_{cc}					
	δ_{ccc}					
		975	7.42	$\nu_{\text{CO}}^{\text{K}}$	$\delta_{\text{cc}=\text{C}}$	

Continued on next page

Table 4 – continued from previous page

V_{IR}^{EXP}	A_{SS}	V_{IR}^{CALC}	A_{CALC}	$\text{km} \cdot \text{mol}^{-1}$	Assignment
		978	23.38	$V_{C-OH}^{Ph_A}$ $V_{C-OH}^{Ph_B}$ $V_{C-OH}^{Ph_{hA}}$ $V_{C-OH}^{Ph_{hB}}$ $V_{C_6C_{12}}^C$	$\delta_{CCC}^{Ph_A}$ $\delta_{CCC}^{Ph_B}$ $\delta_{CCC}^{Ph_B}$ $\delta_{CCC}^{Ph_{hA}}$
		992	123.14	$V_{C_1C_4}^C$ $V_{C_2C_8}^C$ V_{CO}^K $V_{C-OH}^{Ph_A}$ $V_{C-OH}^{Ph_B}$ $V_{CC}^{Ph_{hA}}$ $V_{CC}^{Ph_{hB}}$	$\delta_{CCH}^{Ph_{hA}}$ $\delta_{CCH}^{Ph_{hB}}$ $\delta_{CCH}^{Ph_{hA}}$
1000	ν_{CO}				
	ν_{CC}				
	δ_{CCC}				
		1011	36.54	$V_{C_2C_{34}}^C$ $V_{C_2C_8}^C$ V_{CO}^K	$\delta_{CCH}^{Ph_A}$
		1020	27.33		$\tau_{H^5C_4C_6H_7}$
1022	ν_{CC}	1022	128.61	V_{CC}^S	δ_{COH}^S
	ν_{CO}				
	δ_{CCC}				
	δ_{COH}				
	τ_{HCCH}				

Continued on next page

Table 4 – continued from previous page

$\nu_{\text{IR}}^{\text{EXP}}$	$\nu_{\text{IR}}^{\text{CALC}}$	$\nu_{\text{IR}}^{\text{CALC}}$	$\text{km} \cdot \text{mol}^{-1}$	Assignment
		1022	13.29	$\nu_{\text{CC}}^{\text{S}}$ $\delta_{\text{COH}}^{\text{S}}$
		1029	45.4	$\nu_{\text{CC}}^{\text{S}}$ $\delta_{\text{CCC}}^{\text{P h B}}$ $\tau_{\text{HCCH}}^{\text{S}}$
		1029	5.68	$\nu_{\text{CO}}^{\text{S}}$ $\delta_{\text{COH}}^{\text{S A}}$
		1035	22.96	$\tau_{\text{H}^9\text{C}^8\text{C}^{10}\text{H}^{11}}$
1039	ν_{CC}			
	γ_{COH}			
		1057	61.63	$\nu_{\text{CC}}^{\text{S}}$ $\gamma_{\text{COH}}^{\text{S}}$
		1058	162.87	$\nu_{\text{CC}}^{\text{S}}$ $\gamma_{\text{COH}}^{\text{S}}$
1070	ν_{CO}			
	ν_{CC}			
	δ_{COH}			
	γ_{COH}			
	γ_{CCC}			
		1081	810.56	$\nu_{\text{CC}}^{\text{S}}$ $\delta_{\text{COH}}^{\text{P h B}}$ $\gamma_{\text{COH}}^{\text{S}}$
				$\delta_{\text{COH}}^{\text{P h A}}$
		1082	754.4	ν_{CO} $\gamma_{\text{COH}}^{\text{S}}$
				$\nu_{\text{CO}}^{\text{S}}$
		1088	19.81	$\nu_{\text{CO}}^{\text{S}}$ $\gamma_{\text{CCC}}^{\text{S}}$
		1088	92.81	$\nu_{\text{CO}}^{\text{S A}}$
		1107	57.25	$\delta_{\text{CCH}}^{\text{P h B}}$
				$\delta_{\text{COH}}^{\text{S}}$
				$\delta_{\text{CCH}}^{\text{P h A}}$
				P h B
		1107	4.85	$\nu_{\text{C}_3\text{O}_3\text{O}_8}^{\text{S}}$ δ_{CCH}
		1117	59.47	$\gamma_{\text{CCH}}^{\text{S}}$

Continued on next page

Table 4 – continued from previous page

$\nu_{\text{IR}}^{\text{EXP}}$	$\nu_{\text{IR}}^{\text{CALC}}$	$\nu_{\text{IR}}^{\text{CALC}}$	$\text{km} \cdot \text{mol}^{-1}$	Assignment
	1117	95.78		$\nu_{\text{CO}}^{\text{S}}$ $\delta_{\text{COH}}^{\text{S}}$
				$\nu_{\text{CC}}^{\text{S}}$
	1120	236.02		$\nu_{\text{CO}}^{\text{S}}$
				$\nu_{\text{CC}}^{\text{S}}$
	1121	5.56		$\nu_{\text{CO}}^{\text{S}}$ $\delta_{\text{COH}}^{\text{S}}$
				$\nu_{\text{CC}}^{\text{S}}$ $\delta_{\text{CCH}}^{\text{P hA}}$
				$\delta_{\text{CCH}}^{\text{P hB}}$
1126	ν_{CO}			
	ν_{CC}			
	δ_{CCH}			
	δ_{CCC}			
	γ_{COH}			
	1140	11.97		$\nu_{\text{CC}}^{\text{SB}}$ $\delta_{\text{c2-c34-h35}}$ $\gamma_{\text{COH}}^{\text{S}}$
				$\delta_{\text{CCH}}^{\text{P hA}}$
				$\delta_{\text{CCH}}^{\text{P hB}}$
	1140	35.12		$\delta_{\text{CCH}}^{\text{P hA}}$ $\gamma_{\text{COH}}^{\text{S}}$
				$\delta_{\text{CCH}}^{\text{P hB}}$
	1144	151.56		$\nu_{\text{CC}}^{\text{S}}$ $\delta_{\text{CCH}}^{\text{P hB}}$
				$\nu_{\text{CO}}^{\text{SB}}$
	1144	54.9		$\nu_{\text{CC}}^{\text{SA}}$ $\delta_{\text{CCH}}^{\text{P hA}}$
				$\nu_{\text{CO}}^{\text{SA}}$
	1147	14		$\delta_{\text{CCH}}^{\text{P hB}}$
				$\delta_{\text{CCC}}^{\text{S}}$
				$\delta_{\text{CCO}}^{\text{P hB}}$

Continued on next page

Table 4 – continued from previous page

1
2
3
4
5
6
7
8
9
10
11
12
13
14
15
16
17
18
19
20
21
22
23
24
25
26
27
28
29
30
31
32
33
34
35
36
37
38
39
40
41
42
43
44
45
46
47
48
49
50
51
52
53
54
55
56
57
58
59
60

$\nu_{\text{IR}}^{\text{EXP}}$	$\nu_{\text{IR}}^{\text{CALC}}$	$\nu_{\text{IR}}^{\text{CALC}}$	$\text{km} \cdot \text{mol}^{-1}$	Assignment
		1148	29.77	$\delta_{\text{CCH}}^{\text{ph}_A}$ $\delta_{\text{CCC}}^{\text{S}_A}$ $\delta_{\text{CCO}}^{\text{ph}_A}$
		1160	485.65	$\nu_{\text{C}^2\text{C}^8}$ δ ken c2-c34-c35 $\nu_{\text{C}^2\text{C}^{34}}$ δ c2-c8-h9
		1170	44.38	$\delta_{\text{CCH}}^{\text{ph}_{\text{HB}}}$ $\nu_{\text{CC}}^{\text{S}}$ $\delta_{\text{CCH}}^{\text{ph}_{\text{HB}}}$ $\nu_{\text{CO}}^{\text{S}}$ $\delta_{\text{CCH}}^{\text{ph}_A}$
		1170	32.73	$\nu_{\text{CC}}^{\text{S}}$ $\delta_{\text{CCH}}^{\text{ph}_A}$ $\delta_{\text{CCH}}^{\text{ph}_B}$
1182	ν_{CO}			
	ν_{CC}			
	δ_{CCH}			
	δ_{COH}			
		1196	47.52	$\nu_{\text{C}^{16}\text{O}^{32}}$ $\delta_{\text{CCH}}^{\text{ph}_B}$ $\nu_{\text{C}^6\text{C}^{12}}$ $\delta_{\text{C=CH}}^{\text{K}}$ $\nu_{\text{C}^{10}\text{C}^{21}}$ $\delta_{\text{CCH}}^{\text{ph}_A}$
		1205	27.74	$\nu_{\text{C}^{26}\text{O}^{33}}$ $\delta_{\text{CCH}}^{\text{ph}_B}$ $\nu_{\text{C}^7\text{C}^{12}}$ $\delta_{\text{CCH}}^{\text{ph}_{\text{HA}}}$ $\nu_{\text{C}^7\text{C}^{12}}$ $\delta_{\text{C=CH}}^{\text{K}}$
		1211	21.6	$\delta_{\text{COH}}^{\text{S}}$
		1211	20.04	$\gamma_{\text{COH}}^{\text{S}}$
1216	δ_{CCH}			
		1230	20.25	$\delta_{\text{CCH}}^{\text{ph}_B}$

Continued on next page

Table 4 – continued from previous page

$V_{\text{IR}}^{\text{EXP}}$	A_{ASS}	$V_{\text{IR}}^{\text{CALC}}$	A_{CALC}	$\text{km} \cdot \text{mol}^{-1}$	Assignment
					$\delta_{\text{CCH}}^{\text{p h A}}$
					$\delta_{\text{COH}}^{\text{p h A}}$
					$\delta_{\text{COH}}^{\text{p h B}}$
					δ_{CCH}
1231	90.85				$\delta_{\text{CCH}}^{\text{p h A}}$
					$\delta_{\text{CCH}}^{\text{p h B}}$
					$\delta_{\text{COH}}^{\text{p h A}}$
					$\delta_{\text{COH}}^{\text{p h B}}$
					δ_{CCH}
1237	4.41				$\delta_{\text{CCH}}^{\text{p h A}}$
					$\delta_{\text{CCH}}^{\text{p h B}}$
					$\delta_{\text{COH}}^{\text{p h A}}$
					$\delta_{\text{COH}}^{\text{p h B}}$
					δ_{CCH}
					$\delta_{\text{CCH}}^{\text{s}}$
1238	254.28				$\delta_{\text{CCH}}^{\text{p h B}}$
					$\gamma_{\text{COH}}^{\text{s}}$
					$\delta_{\text{CCH}}^{\text{p h A}}$
					$\delta_{\text{COH}}^{\text{p h A}}$
					$\delta_{\text{COH}}^{\text{p h B}}$
1243	5.18	V_{Cl^4}			δ_{CCH}
		V_{CC}			$\delta_{\text{CCH}}^{\text{p h A}}$
					$\delta_{\text{CCH}}^{\text{p h B}}$
1257	11.02				$\delta_{\text{COH}}^{\text{p h B}}$
					$\delta_{\text{COH}}^{\text{s B}}$

Continued on next page

Table 4 – continued from previous page

1
2
3
4
5
6
7
8
9
10
11
12
13
14
15
16
17
18
19
20
21
22
23
24
25
26
27
28
29
30
31
32
33
34
35
36
37
38
39
40
41
42
43
44
45
46
47
48
49
50
51
52
53
54
55
56
57
58
59
60

$\nu_{\text{IR}}^{\text{EXP}}$	$\nu_{\text{IR}}^{\text{CALC}}$	$\nu_{\text{IR}}^{\text{CALC}}$	$\text{km} \cdot \text{mol}^{-1}$	Assignment
1263	δ_{CCH}	1257	10.31	$\delta_{\text{COH}}^{\text{P h A}}$
				$\delta_{\text{COH}}^{\text{S A}}$
				δ_{CCH}
				ν_{CC}
	ν_{CO}			
1276		1276	15.38	$\delta_{\text{CCH}}^{\text{S A}}$
				$\delta_{\text{COH}}^{\text{S A}}$
1276		1276	42.32	$\delta_{\text{CCH}}^{\text{S B}}$
				$\delta_{\text{COH}}^{\text{S B}}$
1287		1287	73.59	ν_{CC} $\delta_{\text{COH}}^{\text{P hb}}$
				ν_{CO} $\delta_{\text{CCH}}^{\text{P hb}}$
1288		1288	126.87	ν_{CC} $\delta_{\text{COH}}^{\text{P ha}}$
				ν_{CO} $\delta_{\text{CCH}}^{\text{P ha}}$
1290	δ_{COH}	1302	75.84	$\tau_{\text{HCCH}}^{\text{S}}$
				δ_{CCH}
		1302	8.84	
		1303	161.3	δ_{CCH}
		1306	47.21	$\delta_{\text{cch}}^{\text{S}}$
		1306	9.04	$\delta_{\text{COH}}^{\text{S}}$
				$\delta_{\text{cch}}^{\text{S}}$
		1313	59.58	ν_{CO} δ_{CCH}
				$\delta_{\text{COH}}^{\text{K}}$

Continued on next page

Table 4 – continued from previous page

$V_{\text{IR}}^{\text{EXP}}$	A_{ASS}	$V_{\text{IR}}^{\text{CALC}}$	A_{CALC}	$\text{km} \cdot \text{mol}^{-1}$	Assignment
1318	304.38	$V_{\text{CC}}^{\text{P h A}}$	$\delta_{\text{CCH}}^{\text{P h A}}$		
		V_{CO}	$\delta_{\text{COH}}^{\text{P h A}}$		
		$V_{\text{CC}}^{\text{P h B}}$	$\delta_{\text{CCH}}^{\text{P h B}}$		
		V_{CO}	$\delta_{\text{COH}}^{\text{P h B}}$		
1327	117.3	V_{CC}^{K}	$\delta_{\text{COH}}^{\text{K}}$		
		$V_{\text{CC}}^{\text{P h A}}$	$\delta_{\text{CCC}}^{\text{K}}$		
		$V_{\text{CC}}^{\text{P h B}}$	δ_{CCH}		
			$\delta_{\text{COH}}^{\text{P h A}}$		
			$\delta_{\text{COH}}^{\text{P h B}}$		
1352	7.24		δ_{CCH}		
			$\delta_{\text{CCH}}^{\text{P h B}}$		
			$\delta_{\text{COH}}^{\text{P h B}}$		
1354	3.26		δ_{CCH}		
			$\delta_{\text{CCH}}^{\text{P h A}}$		
			$\delta_{\text{COH}}^{\text{P h A}}$		
1355	21.09		$\delta_{\text{CCH}}^{\text{S B}}$		
			$\delta_{\text{COH}}^{\text{S B}}$		
1355	25.84		$\delta_{\text{CCH}}^{\text{S A}}$		
			$\delta_{\text{COH}}^{\text{S A}}$		
1356	598.81	V_{CO}	δ_{CCH}		
		$V_{\text{CC}}^{\text{P h A}}$			
		$V_{\text{CC}}^{\text{P h B}}$			
1365	7.52	V_{CC}	$\delta_{\text{CCH}}^{\text{P h A}}$		
			$\delta_{\text{CCH}}^{\text{P h B}}$		

Continued on next page

Table 4 – continued from previous page

1
2
3
4
5
6
7
8
9
10
11
12
13
14
15
16
17
18
19
20
21
22
23
24
25
26
27
28
29
30
31
32
33
34
35
36
37
38
39
40
41
42
43
44
45
46
47
48
49
50
51
52
53
54
55
56
57
58
59
60

$\nu_{\text{IR}}^{\text{EXP}}$	$\nu_{\text{IR}}^{\text{CALC}}$	$\nu_{\text{IR}}^{\text{CALC}}$	$\text{km} \cdot \text{mol}^{-1}$	Assignment
		1366	26.75	$\delta_{\text{COH}}^{\text{S}}$
		1366	85.98	$\gamma_{\text{COH}}^{\text{S}}$
1371	γ_{CCH}			
	γ_{COH}			
	ν_{CC}			
		1378	84.71	$\gamma_{\text{COH}}^{\text{S}}$
				$\gamma_{\text{CCH}}^{\text{S}}$
		1378	39.33	$\gamma_{\text{COH}}^{\text{S}}$
				$\gamma_{\text{CCH}}^{\text{S}}$
		1392	57.38	ν_{CC}
				$\gamma_{\text{COH}}^{\text{S}}$
				$\gamma_{\text{CCH}}^{\text{S}}$
		1393	52.69	$\delta_{\text{COH}}^{\text{K}}$
				$\gamma_{\text{CCH}}^{\text{S}}$
				δ_{CCH}
		1397	38.43	$\delta_{\text{COH}}^{\text{K}}$
				$\gamma_{\text{CCH}}^{\text{S}}$
				δ_{CCH}
		1400	52.12	$\nu_{\text{C=O}}^{\text{K}}$
				$\delta_{\text{CCH}}^{\text{Ph}_A}$
				$\gamma_{\text{CCH}}^{\text{S}}$
				$\delta_{\text{COH}}^{\text{Ph}_A}$
				δ_{CCH}
				$\delta_{\text{COH}}^{\text{K}}$
1411	ν_{CC}			
	ν_{CO}			
	δ_{COH}			
	δ_{CCH}			
	γ_{CCH}			

Continued on next page

Table 4 – continued from previous page

$V_{\text{IR}}^{\text{EXP}}$	A_{ASS}	$V_{\text{IR}}^{\text{CALC}}$	A_{CALC}	$\text{km} \cdot \text{mol}^{-1}$	Assignment	
1444	δ_{COH} γ_{CCH}	1420	102.44	$\nu_{\text{CO}}^{\text{K}}$ $\nu_{\text{CC}}^{\text{K}}$	$\delta_{\text{COH}}^{\text{K}}$ $\gamma_{\text{CCH}}^{\text{S}_B}$	
		1420	19.39		$\gamma_{\text{CCH}}^{\text{S}_A}$	
		1422	233.8	$\nu_{\text{CO}}^{\text{K}}$ $\nu_{\text{CC}}^{\text{K}}$	$\delta_{\text{COH}}^{\text{K}}$ $\delta_{\text{CCH}}^{\text{K}}$ δ_{CCH} $\delta_{\text{COH}}^{\text{P}_{\text{hb}}}$	$\gamma_{\text{CCH}}^{\text{S}_B}$
		1429	9.21		$\delta_{\text{COH}}^{\text{P}_{\text{h}_A}}$	$\gamma_{\text{CCH}}^{\text{S}_A}$
		1429	9.64		$\delta_{\text{COH}}^{\text{P}_{\text{h}_B}}$	$\gamma_{\text{CCH}}^{\text{S}_B}$
		1449	14.34		$\delta_{\text{COH}}^{\text{P}_{\text{h}_A}}$ $\delta_{\text{COH}}^{\text{P}_{\text{hb}}}$	$\gamma_{\text{CCH}}^{\text{S}_A}$ $\gamma_{\text{CCH}}^{\text{S}_B}$
		1449	10.55		$\delta_{\text{COH}}^{\text{P}_{\text{h}_A}}$ $\delta_{\text{COH}}^{\text{P}_{\text{h}_B}}$	$\gamma_{\text{CCH}}^{\text{S}_A}$ $\gamma_{\text{CCH}}^{\text{S}_B}$
		1460	56.95		$\delta_{\text{COH}}^{\text{P}_{\text{h}_A}}$ $\delta_{\text{COH}}^{\text{P}_{\text{h}_B}}$	$\gamma_{\text{CCH}}^{\text{S}_A}$ $\gamma_{\text{CCH}}^{\text{S}_B}$
		1460	12.89		$\delta_{\text{COH}}^{\text{P}_{\text{h}_A}}$ $\delta_{\text{COH}}^{\text{P}_{\text{hb}}}$	$\gamma_{\text{CCH}}^{\text{S}_A}$ $\gamma_{\text{CCH}}^{\text{S}_B}$
		1463	67.34		$\delta_{\text{COH}}^{\text{P}_{\text{h}_A}}$ $\delta_{\text{COH}}^{\text{P}_{\text{hb}}}$	$\gamma_{\text{CCH}}^{\text{S}_A}$ $\gamma_{\text{CCH}}^{\text{S}_B}$
		1463	6.66		$\delta_{\text{COH}}^{\text{P}_{\text{h}_A}}$ $\delta_{\text{COH}}^{\text{P}_{\text{h}_B}}$	$\gamma_{\text{CCH}}^{\text{S}_A}$ $\gamma_{\text{CCH}}^{\text{S}_B}$
		1478	6.06		$\delta_{\text{COH}}^{\text{P}_{\text{h}_A}}$	$\gamma_{\text{CCH}}^{\text{S}_A}$

Continued on next page

Table 4 – continued from previous page

1
2
3
4
5
6
7
8
9
10
11
12
13
14
15
16
17
18
19
20
21
22
23
24
25
26
27
28
29
30
31
32
33
34
35
36
37
38
39
40
41
42
43
44
45
46
47
48
49
50
51
52
53
54
55
56
57
58
59
60

$\nu_{\text{IR}}^{\text{EXP}}$	$\nu_{\text{IR}}^{\text{CALC}}$	$\nu_{\text{IR}}^{\text{CALC}}$	$\text{km} \cdot \text{mol}^{-1}$	Assignment
				$\delta_{\text{COH}}^{\text{ph}_B}$ $\gamma_{\text{CCH}}^{\text{S}_B}$
	1478	2.26		$\delta_{\text{COH}}^{\text{ph}_A}$ $\gamma_{\text{CCH}}^{\text{S}_A}$
				$\delta_{\text{COH}}^{\text{ph}_B}$ $\gamma_{\text{CCH}}^{\text{S}_B}$
	1488	384.51	$\nu_{\text{CO}}^{\text{K}}$	$\delta_{\text{CCH}}^{\text{K}}$
			$\nu_{\text{CC}}^{\text{K}}$	$\delta_{\text{CCH}}^{\text{ph}_B}$
			$\nu_{\text{CC}}^{\text{ph}_B}$	$\delta_{\text{COH}}^{\text{ph}_B}$
	1499	12.24	$\nu_{\text{CC}}^{\text{ph}_A}$	$\delta_{\text{COH}}^{\text{ph}_A}$
				$\delta_{\text{CCH}}^{\text{ph}_A}$
	1504	262.02	$\nu_{\text{CC}}^{\text{K}}$	$\delta_{\text{COH}}^{\text{K}}$
			$\nu_{\text{CO}}^{\text{K}}$	$\delta_{\text{CCO}}^{\text{K}}$
			$\nu_{\text{CC}}^{\text{ph}_B}$	$\delta_{\text{CCH}}^{\text{ph}_B}$
				$\delta_{\text{COH}}^{\text{ph}_B}$
1508	δ_{HCH}			
	1536	7.1		$\delta_{\text{H}73\text{C}72\text{H}74}$
	1536	9.34		$\delta_{\text{H}78\text{C}77\text{H}79}$
	1555	535.54	$\nu_{\text{CC}}^{\text{ph}_A}$	$\delta_{\text{CCH}}^{\text{ph}_A}$
			$\nu_{\text{CC}}^{\text{ph}_B}$	$\delta_{\text{CCH}}^{\text{ph}_B}$
				$\delta_{\text{COH}}^{\text{ph}_A}$
				$\delta_{\text{COH}}^{\text{ph}_B}$
	1556	22.27	$\nu_{\text{CC}}^{\text{ph}_A}$	$\delta_{\text{CCH}}^{\text{ph}_A}$
			$\nu_{\text{CC}}^{\text{ph}_B}$	$\delta_{\text{CCH}}^{\text{ph}_B}$
				$\delta_{\text{COH}}^{\text{ph}_A}$
				$\delta_{\text{COH}}^{\text{ph}_B}$
1573	δ_{COH}			

Continued on next page

Table 4 – continued from previous page

$V_{\text{IR}}^{\text{EXP}}$	A_{ASS}	$V_{\text{IR}}^{\text{Calc}}$	A_{Calc}	ν_{IR} / $\text{km} \cdot \text{mol}^{-1}$	Assignment
1591	δ_{CCH}	1620	623.04	ν_{CC}	$\delta_{\text{COH}}^{\text{P h}_B}$
				$\nu_{\text{CO}}^{\text{K}}$	δ_{CCH}
				$\nu_{\text{CC}}^{\text{P hB}}$	$\delta_{\text{CCH}}^{\text{P hB}}$
		1626	191.81	$\nu_{\text{CC}}^{\text{P hB}}$	$\delta_{\text{CCH}}^{\text{P hA}}$
					$\delta_{\text{COH}}^{\text{P hA}}$
					δ_{CCH}
1629	ν_{CC}				
	ν_{CO}				
	δ_{CCH}				
	δ_{COH}				
		1631	115.11	ν_{CC}	$\delta_{\text{COH}}^{\text{P hB}}$
				$\nu_{\text{CO}}^{\text{K}}$	δ_{CCH}
				$\nu_{\text{CC}}^{\text{P hB}}$	$\delta_{\text{CCH}}^{\text{P hB}}$
		1652	714.33	$\nu_{\text{CC}}^{\text{K}}$	$\delta_{\text{CCH}}^{\text{K}}$
				ν_{CC}	$\delta_{\text{COH}}^{\text{K}}$
		1664	7.05	$\nu_{\text{CC}}^{\text{P hA}}$	$\delta_{\text{COH}}^{\text{P hA}}$
				$\nu_{\text{C=C}}$	δ_{CCH}
					$\delta_{\text{CCH}}^{\text{P hA}}$
		1666	9.15	ν_{CC}	$\delta_{\text{COH}}^{\text{P hB}}$
				$\nu_{\text{C=O}}^{\text{K}}$	$\delta_{\text{CCH}}^{\text{P hB}}$
					$\delta_{\text{COH}}^{\text{K}}$
		1694	886.87	$\nu_{\text{C=C}}$	$\delta_{\text{COH}}^{\text{K}}$
				ν_{CC}	$\delta_{\text{C=CH}}^{\text{K}}$

Continued on next page

Table 4 – continued from previous page

1
2
3
4
5
6
7
8
9
10
11
12
13
14
15
16
17
18
19
20
21
22
23
24
25
26
27
28
29
30
31
32
33
34
35
36
37
38
39
40
41
42
43
44
45
46
47
48
49
50
51
52
53
54
55
56
57
58
59
60 $V_{\text{IR}}^{\text{EXP}} V_{\text{ASS}} V_{\text{IR}}^{\text{CALC}} V_{\text{A}}^{\text{CALC}} V_{\text{IR}}^{\text{CALC}} \text{ km} \cdot \text{mol}^{-1}$

Assignment

				$\nu_{\text{C=O}}^{\text{K}}$	
				$\nu_{\text{C=C}}^{\text{K}}$	
		1710	46.78	$\nu_{\text{C=C}}$	$\delta_{\text{COH}}^{\text{K}}$
				ν_{CC}	$\delta_{\text{C=CH}}^{\text{K}}$
				$\nu_{\text{C=O}}^{\text{K}}$	
				$\nu_{\text{C=C}}^{\text{K}}$	
	1997	ν_{CC}			
	2053	ν_{CC}			
	2127	ν_{CC}			
	2170	ν_{CO}			
	2296				
	2331				
	2863	ν_{CH}			
	2935	ν_{CH}			
		2943	426.05	$\nu_{\text{CH}}^{\text{K}}$	
	2977	ν_{CH}			
		2984	1.81		
		2984	1.81		
		2989	2.61		
		2990	2.87	$\nu_{\text{CH}}^{\text{S}}$	
		2998	44.62	$\nu_{\text{CH}}^{\text{S}}$	
		2998	63.85	$\nu_{\text{CH}}^{\text{S}}$	
		3026	50.4	$\nu_{\text{CH}}^{\text{S}}$	
		3026	61.7	$\nu_{\text{CH}}^{\text{S}}$	

Continued on next page

Table 4 – continued from previous page

 $\nu_{\text{IR}}^{\text{EXP}} \nu_{\text{IR}}^{\text{CALC}} \nu_{\text{IR}}^{\text{CALC}} \text{ km} \cdot \text{mol}^{-1}$

Assignment

3046	26.37	$\nu_{\text{CH}}^{\text{S}}$
3046	27.24	$\nu_{\text{CH}}^{\text{S}}$
3073	32.19	$\nu_{\text{CH}}^{\text{S}}$
3073	22.72	$\nu_{\text{CH}}^{\text{S}}$
3077	35.93	$\nu_{\text{CH}}^{\text{S}}$
3077	50.39	$\nu_{\text{CH}}^{\text{S}}$
3177	0.1	ν_{CH}
3186	12.25	ν_{CH}
3188	0.11	ν_{CH}
3197	11.89	ν_{CH}
3207	3.83	$\nu_{\text{CH}}^{\text{P}^{\text{h}}}$
3207	3.48	$\nu_{\text{CH}}^{\text{P}^{\text{h}}}$
3209	6.39	$\nu_{\text{CH}}^{\text{P}^{\text{h}}}$
3209	5.41	$\nu_{\text{CH}}^{\text{P}^{\text{h}}}$
3222	4.73	$\nu_{\text{CH}}^{\text{P}^{\text{h}}}$
3222	1.11	$\nu_{\text{CH}}^{\text{P}^{\text{h}}}$
3223	18.14	$\nu_{\text{C}34\text{-H}35}$
3567	947.75	$\nu_{\text{O}32\text{-H}83}$
3569	589.9	$\nu_{\text{O}33\text{-H}82}$
3724	54.31	$\nu_{\text{OH}}^{\text{S}}$
3724	67.51	$\nu_{\text{OH}}^{\text{S}}$
3726	54.7	$\nu_{\text{OH}}^{\text{S}}$
3726	36.68	$\nu_{\text{OH}}^{\text{S}}$
3742	69.03	$\nu_{\text{OH}}^{\text{S}}$

Continued on next page

Table 4 – continued from previous page

$\nu_{\text{IR}}^{\text{EXP}}$	$\nu_{\text{IR}}^{\text{CALC}}$	$\nu_{\text{IR}}^{\text{CALC}}$	Assignment
	3742	59.96	$\nu_{\text{OH}}^{\text{S}}$
	3766	24.08	$\nu_{\text{OH}}^{\text{S}}$
	3766	32.37	$\nu_{\text{OH}}^{\text{S}}$

For Peer Review

1
2
3
4
5
6
7
8
9
10
11
12
13
14
15
16
17
18
19
20
21
22
23
24
25
26
27
28
29
30
31
32
33
34
35
36
37
38
39
40
41
42
43
44
45
46
47
48
49
50
51
52
53
54
55
56
57
58
59
60

For Peer Review

How glucosylation triggers physical-chemical properties of Curcumin: an experimental and theoretical study

Rois Benassi*, Erika Ferrari, Sandra Lazzari, Francesca Pignedoli, Ferdinando Spagnolo, Monica Saladini
Department of Chemistry, University of Modena and Reggio Emilia, via Campi 183, 41100 Modena, Italy

Abstract

In the present study we investigate the structures of glucosylated curcumin derivatives with DFT at B3LYP/6-31G* level. A conformational analysis is performed in order to determine the GS (conformational minimum) and TS (rotational transition state) of curcumin derivatives and then their electronic features are evaluated. HOMO and LUMO frontier orbitals and Maps of Electron Density Potential (MEPs) are plotted and compared. In order to correlate their predicted spectroscopic properties with IR, UV-vis and NMR experimental data we extended the theoretical study on electronic properties to different solvents (H₂O, MeOH, ACN, DMSO). The main finding is that the curcuminic core maintains the same geometrical and electronic structures in all compounds miming the metal coordination capability showed by curcumin. Therefore we may confirm that the presence of glucose does not affect the electronic properties of the derivatives.

Keywords: *Curcumin, DFT, β -keto-enolic structure, glucosyl-curcuminoids*

*Corresponding author: tel +39 0592055046, Fax +39 059373543, e-mail: rois.benassi@unimore.it

1. Introduction

Curcumin (1,7-bis(4-hydroxy-3-methoxyphenyl)-1,6-heptadiene-3,5-dione), a yellow spice extracted from *Curcuma Longa* L. rhizomes, is used in a wide range of applications, from industrial dyes to pharmaceutical treatments.^[1-3] It is proved that curcumin holds selective metal-chelating properties that are pharmaceutically interesting.^[4] In the field of medicinal chemistry one of the most promising properties of curcumin is its metal ligating ability towards Gallium and Iron.^[5,6] This feature can be exploited for a variety of pharmaceutical aims like metal overload detoxification, metal delivery and radio imaging. Despite these potential pharmaceutical applications, curcumin has a low water solubility and limited bioavailability that makes it difficult to handle for pharmaceutical use. To improve chemical properties of curcumin, several derivatives were synthesized and studied by means of theoretical and experimental data.^[7,8] The glucosylation of the aromatic ring was found to enhance curcumin water-solubility and kinetic stability which is a fundamental feature for drug bioavailability.^[9] The compounds were characterized and their ability to act as metal-chelating agents was also evaluated.^[9,10] Biological properties of these molecules were also tested and they showed cytotoxicity towards human ovarian carcinoma cell line leading to an improvement of *Cisplatin* efficiency with higher selectivity towards cancer than non-cancer cells.^[11] In order to elucidate chemical-physical properties of these molecules and to correlate their electronic structures with the ability to act as metal chelating agents, in the present study we employ DFT calculations for a conformational analysis of the compounds reported in **Figure 1**. A full optimization of the geometry is followed by a conformational search in order to study the potential energy surface (PES) as a function of the rotation of the O-C exocyclic dihedral angle (ϕ) (**Figure 1**). It was reported that the presence of different solvents perturbs intra- or inter-molecular hydrogen bonds in curcumin modifying its photophysical behavior.^[12] Therefore now we perform also a theoretical study on the electronic properties of glucosyl-curcuminoids in different solvents in order to correlate their predicted spectroscopic properties with IR, UV-vis and NMR experimental data.

2. Methods

2.1 Computational details

The computations of all the studied compounds were performed by the DFT approach. The structures were fully optimized using hybrid-functional B3LYP applied to 6-31G* basis set (B3LYP/6-31G*)^[13-15] by means of Gaussian 03^[16] package of programs.

In a previous study we described curcumin structure using both B3LYP/6-311G** and B3LYP/6-31G* levels.^[17] By comparing the obtained results, B3LYP/6-31G* showed to be a good compromise between accuracy and precision. All the calculated properties agreed well with those obtained using B3LYP/6-311G**. Therefore we decided to employ B3LYP/6-31G* in order to study the influence of glucosylation on curcumin properties. GaussView 03^[18] was used as a plotting tool for data visualization.

Thermodynamics were obtained from vibrational analysis employing general procedures. The analysis of the calculated vibrational properties always confirmed the conformational minimum (GS) or rotational transition state (TS), characterized as a saddle point, for the considered structure.

Atom charges were calculated from the optimized geometries at B3LYP/6-31G* level with the CHELPG approach as implemented in Gaussian 03. The molecular electrostatic potential maps (MEPs) were plotted by Gaussview and reported onto 0.02 e/Bohr isosurface of electron density; representations of HOMO and LUMO orbital density were referred to an isovalue of 0.0004.

The solvent effects were evaluated by employing the self-consistent reaction field (SCRF) method with polarized continuum model (PCM).^[19-21]

The absorption wavelengths and oscillator strengths were calculated by means of time-dependent density functional theory (TD-DFT) as implemented in Gaussian 03. The magnetic isotropic shielding tensors (σ) for ¹H and ¹³C NMR were calculated using the standard GIAO

1
2
3 (Gauge-Independent Atomic Orbital) ^[22] at B3LYP/6-31G* approach with the Gaussian 03 program
4
5 package.
6
7
8
9

10 2.2 Conformational analysis

11
12 Starting with the mono glucosyl-compounds, Series **A** (**Figure 1**), all structures were fully
13 optimized with the DFT approach at B3LYP/6-31G* level.
14

15
16 We utilized the geometries of the full reoptimized structures as the starting point for a rigid
17 PES scan of the O-C exocyclic dihedral angle (ϕ) (**Figure 1**). The dihedral angle ϕ was rotated at
18
19 15° step size up to a complete 360° turn.
20
21
22
23

24
25 Minimum and maximum points on rigid PES were optimized and characterized as GS and
26
27 TS states from the vibrational analysis. For all structures the starting point was confirmed to be the
28
29 most stable structure.
30

31
32 Geometry of compounds **C** (**Figure 1**) was built from the more stable structure of the
33
34 corresponding series **A**, adding a second glucose molecule. All the possible dispositions of the
35
36 second sugar molecule with respect to curcumin planar skeleton were examined and optimized.
37
38 Calculations on **C** compounds were then run using the same approach (rigid PES search of ϕ
39
40 dihedral angle, optimization of the obtained structures, vibrational analysis, CHELPG charges
41
42 calculation, plots of HOMO and LUMO molecular orbitals and MEPs).
43
44
45
46
47

48 2.2 Spectroscopy

49
50 Spectroscopic data were collected only for previously synthesized compounds **C**.^[10]
51

52
53 NMR spectra were recorded at 300 K on a Bruker Avance AMX-400 spectrometer with a
54
55 Broad Band 5 mm probe (inverse detection). Nominal frequencies were 100.13 MHz for ¹³C and
56
57 400.13 MHz for ¹H. The typical acquisition parameters for ¹H were as follows: 20 ppm spectral
58
59 bandwidth (SW), 6.1 μ s pulse width (90° pulse hard pulse on ¹H), 0.5-1 s pulse delay, 216-512
60

number of scans. For 2D H,H-Homonuclear Correlated Spectroscopy (COSY)^[23] typical parameters were used. For 2D H,X-Hetero Correlated Spectroscopy (HMBC^[24] and HMQC^[25]) opportune parameters were used (50-90° pulses; 32k data points; 1 s relaxation delay; 8-64k transients; ¹J_{H-C} 125-145 Hz; ³J_{H-C} 5-15 Hz). Methanol-*d*₄ (MeOD) and DMSO-*d*₆ (DMSO) were used as NMR solvents. D₂O spectra showed line broadening due to hydrogen bond network forbidding their assignment.

UV-Vis measurements were performed using Jasco V-570 spectrophotometer at 25.0 ± 0.1°C in the 200-600 nm spectral range employing a 1 cm quartz cell. 2.5 × 10⁻⁵ M solutions were prepared using different solvents: H₂O, ACN, DMSO and MeOH.

The infrared spectra of solid compounds were obtained by means of a Bruker FTIR VERTEX 70, with a MCT Mid-Band detector in the 4000-600 cm⁻¹ spectral range using an ATR Golden-Gate (Heated-Diamond top-plate).

3. Results and discussion

3.1. Conformational analysis

Previous studies^[7,17,26] demonstrated that the keto-enolic tautomer of curcumin is the most stable form, so that we decided to use it to describe the core of all curcumin derivatives reported in **Figure 1**.

The first remarkable result is that for all compounds the curcuminic core maintains a completely planar conformation with the same geometrical parameters as curcumin.^[17] allowing Curcumin-like electronic conjugation of aromatic/ π electrons. This was found to be a fundamental feature to allow metal coordination through dissociated enolic moiety.^[27] The introduction of a glucose molecule may perturb curcumin skeleton by means of hydrogen bond interactions or conjugation effects, therefore we decided to scan the dihedral angle ϕ as it defines the sugar

1
2
3 molecule orientation. **Table 1** reports energies, thermodynamic quantities and dihedral angles (ϕ , θ)
4
5 values obtained from conformational analysis of all studied compounds.
6
7

8 A plot of ΔG values as a function of ϕ angle for **A** type compounds is reported in **Figure 2**.

9
10 From the analysis of rotational free energy, two states of rotational maximum (TS_1 and TS_2) and
11
12 two states of minimum (GS_1 and GS_2) are found.

13
14 The main differences in ϕ values are observed for the absolute minimum conformation
15
16 (GS_1), ranging from 71° to 118° (**Table 1**). The ϕ value increases following the decrease of
17
18 aromatic substituent steric hindrance ($H<OH<OCH_3$). GS_2 ground state is less influenced by
19
20 substituent bulkiness, since the sugar moiety is rotated thus minimizing the interaction with the
21
22 substituent on the aromatic ring (**Figure 3**). As a consequence, ϕ values in GS_2 are similar, ranging
23
24 from 282° to 293° .
25
26
27
28
29

30 Free activation energies of rotation (ΔG^*) of TS_1 for **A2** and **A3** are similar (**A2** 7.67 kcal
31
32 mol^{-1} ; **A3** 7.45 kcal mol^{-1}), while for **A1** ΔG^* assumes an higher value (9.43 kcal mol^{-1}). In **A1** the
33
34 geometrical analysis of GS_1 (**Figure 3**) provides evidence for a hydrogen bond between OH
35
36 phenolic group and a hydroxylic oxygen atom of the sugar moiety (O33-H60...O49 1.96 Å, O-H...O
37
38 angle 158.6°). The hydrogen bond break in **A1** strongly contributes to the higher ΔG^* . In **A2** and
39
40 **A3** only steric effects are responsible for the ΔG^* value and no evidence of significant H-bond is
41
42 observed. Previous study on similar β -diketo-mono-glucosylated derivatives ^[27] showed the
43
44 formation of a hydrogen bond involving OCH_3 aromatic substituent and glucosydic moiety (OH...O
45
46 2.23 Å, OHO angle 155°). Instead in **A2**, no hydrogen interaction is observed suggesting that the
47
48 greater extent of π delocalization with respect to the previously studied compound, probably makes
49
50 OCH_3 group less capable to form a hydrogen bond.
51
52
53
54
55

56 In di-glucosylated compounds **C**, all the possible dispositions of the two sugar moieties with
57
58 respect to the planar skeleton of curcumin were optimized and the results for **C2** are reported in
59
60

1
2
3 **Figure 4, C1 and C3** show the same trend. The *syn-syn* configuration is the most stable therefore it
4
5 is used as the starting point for conformational analysis on ϕ dihedral angle. For all compounds **C**
6
7 the value of the θ dihedral angle results close to the corresponding ϕ angle in GS_1 state of
8
9 compounds **A** with opposite sign.
10
11

12
13 Compounds **C** show the same trend as mono-glucosylated series **A** regarding PSE. The ΔG^*
14
15 and dihedral angles for **A** and **C** homologues are superimposable with a maximum difference of $\pm 2^\circ$
16
17 (**Table 1**).
18
19

20 For each compound **C**, in all states of maximum and minimum, the value of the not scanned
21
22 θ dihedral angle is constant and equal to the ϕ value obtained in the ground state (GS_1) with
23
24 opposite sign. This evidence suggests that the two sugar molecules rotate independently and do not
25
26 influence each other during the rotation. We suggest that θ angle can rotate with the same potential
27
28 energy as ϕ since compounds **C** maintain the same symmetric structure observed in curcumin. For
29
30 all compounds the relatively low ΔG^* values ($< 10.04 \text{ kcal mol}^{-1}$) allow a “free” rotation of the
31
32 glucosydic group around ϕ and θ dihedral angle at room temperature. Anyway the free rotation of
33
34 the glucose moieties does not exert any steric hindrance on keto-enolic group in any conformation,
35
36 maintaining it accessible to a metal ion for the coordination reaction.
37
38
39
40

41 We observed also the formation of a hydrogen bond interaction between the OH phenolic
42
43 group and the sugar moiety (O33-H82...O56 1.96 Å, O-H...O angle 158.7°) in **C1**. In a previous
44
45 study on compounds **C** we discovered that the nature of a *meta* substituent on the aromatic ring
46
47 affects its lipophilicity in the order $\text{OH} > \text{H} > \text{OCH}_3$ [10] Today computational data may account for the
48
49 unexpected increased lipophilicity of **C1** due to the formation of an intra-molecular hydrogen bond
50
51 with the glucosydic moiety.
52
53
54
55
56
57
58
59
60

3.2. Molecular Orbitals

HOMO and LUMO molecular orbitals were calculated for both GS and TS conformers for **A** and **C** series. **Figure 5** shows HOMO and LUMO molecular orbitals at the GS₁ conformation, HOMO and LUMO for the other conformations GS₂, TS₁, TS₂ are perfectly overlapping with GS₁. HOMO and LUMO are delocalized through the whole curcuminic core, allocating the electron density both on the dienic and benzenic moieties as found for curcumin.^[17,26] The introduction of one or two glucose molecules does not add any interaction between the newly attached substituent and the aromatic groups, thus not affecting the peculiar conjugation of aromatic/ π electrons of curcumin core confirming the results of conformational analysis.

3.3 MEPs

Figure 6 shows the MEPs of GS₁ states. In all compounds, the negative charge of the curcuminic core is located on the β -keto-enolic oxygen atoms, resembling the same trend of curcumin.^[17,26] **Table 2** reports charge density values of β -keto-enolic and phenolic oxygen atoms of **A1** and **C1** in GS₁ state. By comparing the values obtained in *vacuum* with those of curcumin we can observe variation of ≈ 0.004 in the negative charge of the β -keto-enolic oxygen atoms, thus suggesting the same potential metal coordination ability of curcumin.^[6] The presence of OH groups in **A1** and **C1** introduces a further center of negative charge that might affect their physical-chemical properties. Although enolic and phenolic oxygens show almost the same negative charge values the involvement of phenolic oxygen in metal coordination is prevented by the higher pK_a value [pK_a (phenolic) 9.4; pK_a (enolic) 8.2].^[11] The negative charge on OH aromatic substituent evidences its strong electron withdrawing ability, which probably influences the pK_a value of the β -keto-enolic group. In fact **C1** was found to be the most acidic compound in aqueous solution and the more effective Fe(III) and Ga(III) chelating agent.^[11]

Compounds **A** and **C** show the same electronic properties (MEPs, CHELPG) suggesting similar coordination ability. Therefore the analysis of solvent effects is limited to **C** compounds in

1
2
3 order to compare their electronic properties with experimental data. MEPs calculated in different
4
5 solvents look like those in *vacuum*; the corresponding density charge values are reported in **Table 2**.
6
7

8 We can observe a general increase in the negative charge on ketonic oxygen atom in
9
10 solvents with respect to *vacuum*. This effect seems to be directly related to the solvent polarity. In
11
12 fact H₂O gives the major increase in negative charge. On the contrary the ability to form hydrogen
13
14 bonds seems not to influence charge distribution. The high charge density on the enolic function
15
16 may account for the replacement of hydrogen atom by metal ion with a lower pK_a value with
17
18 respect to free ligand system, enabling metal coordination and preventing hydroxide precipitation.
19
20
21

22 MEPs do not take into account higher electrostatic effects than polarization which may be
23
24 very important in metal complexation. Anyway the higher charge density on keto-enolic group with
25
26 respect to sugar oxygen atoms suggests that the keto-enolic function is the only group potentially
27
28 involved in metal coordination. In addition to the chelating effect, the enolic proton acidity enforces
29
30 this assumption. Previous NMR study on compounds **C** ^[9] established that sugar moiety was never
31
32 involved in metal ligation as no ¹H and ¹³C chemical shifts were observed upon metal addition.
33
34
35
36
37
38

39 3.3 NMR spectroscopy

40 ¹H and ¹³C NMR spectra of compounds **C** were recorded and compared with the calculated
41
42 values. **Figure 7** reports ¹H NMR spectrum of **C1** in DMSO-*d*₆. Experimental data evidence only
43
44 one set of signals corresponding to the keto-enolic form; the complete symmetry (C_{2v}) of the
45
46 molecule, due to resonance between the two possible keto-enolic limiting structures, is supported by
47
48 the equivalence of double bonds and aromatic rings, and by ¹³C NMR spectrum giving
49
50 undistinguishable and equivalent peaks for ketonic and enolic carbons. **C2** and **C3** behave similarly.
51
52 The fit between experimental chemical shifts of glucosyl-curcuminoids in DMSO and MeOD for
53
54 both ¹H (**Figure 8A**) and ¹³C (**Figure 9B**) illustrates the very small variations due to experimental
55
56 conditions.
57
58
59
60

1
2
3 The GIAO (Gauge-Independent-Atomic-Orbitals) isotropic magnetic shielding tensors (σ_{calc})
4 were calculated for **C1**, **C2** and **C3** in *vacuum*, H₂O, MeOH, and DMSO (**Table 1-3**, supplementary
5 material). Bearing in mind the experimental molecular symmetry of glucosyl-curcuminoids, the
6 average value of σ_{calc} ($\bar{\sigma}_{calc}$) between the two keto-enolic limit structures was calculated and
7 reported in **Table 3** for each solvent system.
8
9

10
11
12
13
14
15
16 ¹³C and ¹H experimental chemical shift assignments were supported by 2D COSY, HSQC
17 and HMBC experiments. The data are reported in **Table 4** and **Table 5**.

18
19
20 Plotting the experimental ¹³C and ¹H chemical shifts (δ_{exp}) in MeOD and DMSO *versus* the $\bar{\sigma}_{calc}$ in
21 *vacuum* or in the same solvent system, a linear regression is observed: $\delta_{exp} = a \cdot \bar{\sigma}_{calc} + b$ (a, b and R²
22 parameters are given in **Table 4** and **Table 5**). This relationship is then used to predict the chemical
23 shifts (δ_{pred}).^[17,28] As already observed,^[29] the correlation between experimental chemical shifts and
24 calculated isotropic screening constants is better for ¹³C than for ¹H. In fact the correlation
25 coefficient R² ranges from 0.9834 to 0.9939 for ¹³C and from 0.9186 to 0.9718 for ¹H.
26
27

28
29
30
31
32
33
34
35 A comparison with previously reported Curcumin predicted ¹³C NMR data^[18] highlights
36 how for glucosyl-curcuminoids the presence of the sugar moiety experiences the solvent effect; in
37 fact linear regressions are definitely better when calculated on the basis of $\bar{\sigma}_{calc}$ in the same solvent
38 system than *in vacuum*.
39
40
41
42
43
44

45
46 ¹H δ_{pred} values (**Table 5**) provide good correlation with δ_{exp} with exception of H-1, due to
47 the fact that the GIAO σ_{calc} has almost the same value in the two resonance limit structures of keto-
48 enolic moiety. As a consequence electronic delocalization cannot be predicted accurately. **Table 5**
49 data confirm the importance of the solvent environment in predicting correct ¹H δ_{pred} ; in fact the gap
50 in R² value between *in vacuum* and solvent prediction is higher for ¹H (0.0117-0.0319) than ¹³C
51 (0.0003-0.0044).
52
53
54
55
56
57
58
59
60

ΔR^2 values ($R^2_{\text{solvent}} - R^2_{\text{vacuum}}$) prove that the solvent has a greater effect in **C1** and **C2** than in **C3**; ^1H NMR data of **C1** are better predicted in MeOH than in DMSO, **C3** behaves in the opposite way while for **C2** the two solvents show the same effect. This behavior suggests that the OH and OCH_3 groups in **C1** and **C2** respectively may interact with the solvent through hydrogen bond and/or dipolar interactions.

Figure 9 reports the plotting of ^1H and ^{13}C δ_{exp} vs. $\bar{\sigma}_{\text{calc}}$ for **C1** together with the linear relationships. **C1** behaves differently from **C2** and **C3** as it concerns anomeric proton (H-11), in fact this proton is not well predicted by calculation as a consequence of the intra-molecular hydrogen bond between the OH phenolic group and the sugar moiety.

3.4. UV-Vis spectroscopy

Each compound shows a strong intense absorption band in the 300-500 nm wavelength region. Absorption maxima are reported in **Table 6** together with calculated values in the corresponding solvent. The red shift in DMSO with respect to ACN medium follows the order **C1**>**C2**>**C3** and it is related to the higher polarity of the phenolic substituent (OH > OCH_3 > H) interacting with different polar solvents. A solvent dependent red shift in maximum was found also in curcumin ^[12] and was related to solvent polarity and proticity. In fact methanol, a strong hydrogen bond-donating as well as hydrogen bond accepting solvent gave the greatest maximum red shift. In our case the three compounds in H_2O and MeOH behaves similarly, probably because the hydrogen bond effect is masked by the presence of sugar moiety. The same trend is observed in the predicted values.

3.5 Infra Red Spectroscopy

Usually the calculated harmonic vibrational wavenumbers are higher than the experimental ones, because of the anharmonicity, incomplete treatment of electron correlation and use of finite

1
2
3 one-particle basis set.^[29] A linear relationship with a good correlation coefficient is obtained
4
5 plotting the experimental wavenumbers *versus* the calculated ones ($\bar{\nu}_{\text{calc}}$) for all compounds **C**;
6
7
8 **Figure 10** reports **C1** data. This result suggests that the over-estimation of calculated wave numbers
9
10 is quite systematic and allows to predict FT-IR spectra. The slope of the linear regression ($a=$
11
12 0.9991) is greater than the value (0.9613) estimated at B3LYP/6-31G* level for a great number of
13
14 different compounds.^[30] A list of the experimental and calculated frequencies together with a
15
16 tentative assignment is reported as supplementary material (Table 4 supplementary material)
17
18
19
20
21

22 Conclusions

23
24 We have demonstrated that the addition of bulky sugar groups does not affect the
25
26 electronic properties of the curcuminic core, allowing metal coordination through keto-enolic
27
28 moiety. A glucose moiety interacts only with meta-substituents on the aromatic ring influencing its
29
30 lipophilicity.
31
32

33
34 The solvent effect is a critical aspect in predicting spectroscopic data which well agree with
35
36 the experimental ones.
37
38
39
40

41 Acknowledgments

42
43 We are thankful to the “Consorzio Interuniversitario per il Calcolo Automatico dell'Italia
44
45 Nord Orientale - CINECA” and to the “Laboratorio di Calcolo Scientifico Avanzato
46
47 Interdipartimentale dell'Università degli Studi di Modena e Reggio Emilia” for computing facilities.
48
49 We are grateful to the “Centro Interdipartimentale Grandi Strumenti – C.I.G.S.” of the University of
50
51 Modena and Reggio Emilia and to the “Fondazione Cassa di Risparmio di Modena” for supplying
52
53 NMR spectrometer.
54
55
56
57
58
59
60

References

1. S. Goel, B. Jhurani, B. Aggarwal, *Mol. Nutr. Food Res.* **2008**; 52, 1010.
2. R.A. Sharma, A.J. Gescher, W.P. Steward, *Eur. J. Cancer* **2005**; 4, 1955.
3. R.K. Maheshwari, A.K. Singh, J. Gaddipati, R.C. Srimal, *Life Sci.* **2006**; 78, 2081.
4. L. Shen, H.F. Ji, *Spectrochim. Acta A Mol. Biomol. Spectrosc.* **2007**; 67,619.
5. Y. Jiao, J. Wilkinson IV, X. Di, W. Wang, H. Hatcher, N.D. Kock, R. D'Agostino Jr, M.A. Knovich, F.M. Torti, S.V. Torti, *Blood* **2009**; 113 462.
6. M. Borsari, E. Ferrari, R. Grandi, M. Saladini, *Inorg. Chim. Acta* **2002**; 328, 61.
7. P. Cornago, R.M. Claramount, L. Bouissane, I. Alkorta, J. Elguero, *Tetrahedron* **2008**; 8089.
8. V. Bertolasi, V. Ferretti, P. Gilli, X. Yao, C. J. Li, *New J. Cem.* **2008**; 32, 694.
9. B. Arezzini, M. Ferrali, E. Ferrari, R. Grandi, S. Monti, M. Saladini, *Eur. J. Inorg. Chem.* **2004**; 3, 646.
10. E. Ferrari, B. Arezzini, M. Ferrali, S. Lazzari, F. Pignedoli, F. Spagnolo, M. Saladini, *BioMetals* **2009**; 22, 701.
11. E. Ferrari, S. Lazzari, G. Marverti, F. Pignedoli, F. Spagnolo, M. Saladini, *Biorg. Med. Chem.* **2009**; 17, 3043.
12. S.M. Khopde, K.I. Priyadarsini, D.K. Palit, T. Mukherjee, *Photochem. Photobiol.* **2000**; 72 , 625.
13. B. Miehllich, A. Savin, H. Stoll, H. Preuss, *Chem. Phys. Lett.* **1989**; 157, 200.
14. W. Lee, R. Yang, G. Parr, *Phys. Rev.* **1988**; B 37, 785.
15. A.D. Becke, *J. Chem. Phys.* **1993**; 98, 5648.
16. M.J. Frisch, G.W. Trucks, H.B. Schlegel, G.E. Scuseria, M.A. Robb, J.R. Cheeseman, J.A. Montgomery Jr., T. Vreven, K.N. Kudin, J.C. Burant, J.M. Millam, S.S. Iyengar, J. Tomasi, V. Barone, B. Mennucci, M. Cossi, G. Scalmani, N. Rega, G.A. Petersson, H. Nakatsuji, M. Hada, M. Ehara, K. Toyota, R. Fukuda, J. Hasegawa, M. Ishida, T. Nakajima, Y. Honda, O. Kitao, H. Nakai,

- 1
2
3 M. Klene, X. Li, J.E. Knox, H.P. Hratchian, J.B. Cross, V. Bakken, C. Adamo, J. Jaramillo, R.
4
5 Gomperts, R.E. Stratmann, O. Yazyev, A.J. Austin, R. Cammi, C. Pomelli, J.W. Ochterski, P.Y.
6
7 Ayala, K. Morokuma, G.A. Voth, P. Salvador, J.J. Dannenberg, V.G. Zakrzewski, S. Dapprich,
8
9 A.D. Daniels, M.C. Strain, O. Farkas, D.K. Malick, A.D. Rabuck, K. Raghavachari, J.B. Foresman,
10
11 J.V. Ortiz, Q. Cui, A.G. Baboul, S. Cliord, J. Cioslowski, B.B. Stefanov, G. Liu, A. Liashenko, P.
12
13 Piskorz, I. Komaromi, R.L. Martin, D.J. Fox, T. Keith, M.A. Al-Laham, C.Y. Peng, A.
14
15 Nanayakkara, M. Challacombe, P.M.W. Gill, B. Johnson, W. Chen, M.W. Wong, C. Gonzalez, J.A.
16
17 Pople, *Gaussian 03*, Revision C.02, Gaussian, Inc., Wallingford, CT, **2004**.
18
19
20
21
22 17. R. Benassi, E. Ferrari, S. Lazzari, F. Spagnolo, M. Saladini, *J. Mol. Struct.* **2008**; 892, 168.
23
24 18. R. Dennington II, T. Keyth, J. Millam, K. Eppinnett, W.L. Hovell, R. Gilliland, *Gaussview*,
25
26 *Version 3.0*, Semichem, Inc., Shawnee Mission, KS, **2003**.
27
28
29 19. S. Miertus, E. Scrocco, J. Tomasi, *Chem. Phys.* **1981**; 55, 117.
30
31 20. S. Miertus, J. Tomasi, *Chem. Phys.* **1982**; 65, 239.
32
33 21. M. Cossi, V. Barone, Cammi, J. *Chem. Phys. Lett.* **1996**; 255, 327.
34
35 22. K. Wolinski, J.F. Hinton, P.J. Pulay, *J. Am. Chem. Soc.* **1990**; 112, 8251.
36
37 23. K. Nagayama, A. Kumar, K. Wuethrich, R.R. Ernst, *J. Magn. Res.* **1980**; 40, 321.
38
39 24. A. Bax, M.F. Summers, *J. Am. Chem. Soc.* **1986**; 108, 2093.
40
41 25. A. Bax, R. H. Griffey, B. L. Hawkins, *J. Magn. Res.* **1983**; 55, 301.
42
43 26. E. Benassi, F. Spagnolo, *Theor. Chem. Acc.* **2009**; 124, 235.
44
45 27. R. Benassi, E. Ferrari, R. Grandi, S. Lazzari, M. Saladini, *J. Inorg. Biochem.* **2007**; 101, 203.
46
47 28. Blanco, I. Alkorta, J. Elguero, *Magn. Res. Chem* **2007**; 45, 797.
48
49 29. F. M. Szafran, E. Bartoszak-Adamska, J. Koput, Z. Dega-Szafran, *J. Mol. Struct.* **2007**; 140,
50
51 844.
52
53 30. J.B. Foresman, A. Frisch, "Exploring Chemistry with Electronic Structure Methods: A Guide
54
55 to Using Gaussian"(2 ed.), Gaussian, Inc, Pittsburgh, PA **1996**.
56
57
58
59
60

Table 1- θ and ϕ dihedral angles, total electronic energies (E), zero point vibrational energies (E + ZPE), thermodynamic quantities (G, H) and relative differences calculated at B3LYP/6-31G*.

a) Not rotated dihedral angle; b) rotated dihedral angle; c) a.u. ; d) kcal mol⁻¹

State	θ^a	ϕ^b	E ^c	E+ZPE ^c	H ^c	G ^c	ΔE^d	$\Delta E+ZPE^d$	ΔH^d	ΔG^d
A1 GS ₁	-	99.89	-1795.689556	-1795.202059	-1795.166855	-1795.272771	0.00	0.00	0.00	0.00
TS ₁	-	203.03	-1795.675170	-1795.188357	-1795.153763	-1795.257743	9.03	8.60	8.22	9.43
GS ₂	-	282.23	-1795.685569	-1795.198340	-1795.162987	-1795.269849	2.50	2.33	2.43	1.83
TS ₂	-	358.46	-1795.675225	-1795.188406	-1795.153778	-1795.257568	8.99	8.57	8.21	9.54
A2 GS ₁	-	71.35	-1874.295775	-1873.750883	-1873.712800	-1873.826631	0.00	0.00	0.00	0.00
TS ₁	-	216.94	-1874.286710	-1873.742105	-1873.704899	-1873.814405	5.69	5.51	4.96	7.67
GS ₂	-	293.57	-1874.293078	-1873.747762	-1873.709895	-1873.822106	1.69	1.96	1.82	2.84
TS ₂	-	347.61	-1874.288686	-1873.744054	-1873.706854	-1873.816857	4.45	4.29	3.73	6.13
A3 GS ₁	-	117.93	-1645.248964	-1644.770062	-1644.737057	-1644.839474	0.00	0.00	0.00	0.00
TS ₁	-	215.56	-1645.238652	-1644.760269	-1644.728023	-1644.827595	6.47	6.15	5.67	7.45
GS ₂	-	285.75	-1645.247768	-1644.768673	-1644.735734	-1644.838272	0.75	0.87	0.83	0.75
TS ₂	-	354.04	-1645.240588	-1644.762127	-1644.729889	-1644.829315	5.26	4.98	4.50	6.37
C1 GS ₁	-100.42	100.33	-2406.423034	-2405.761907	-2405.715397	-2405.848672	0.00	0.00	0.00	0.00
TS ₁	-100.76	203.85	-2406.408721	-2405.748111	-2405.702281	-2405.832897	8.98	8.66	8.23	9.90
GS ₂	-100.38	283.45	-2406.419166	-2405.757980	-2405.711444	-2405.843949	2.43	2.46	2.48	2.96
TS ₂	-101.45	358.72	-2406.408670	-2405.748086	-2405.702199	-2405.832666	9.01	8.67	8.28	10.04
C2 GS ₁	-70.29	70.21	-2485.008984	-2484.291502	-2484.241500	-2484.383139	0.00	0.00	0.00	0.00
TS ₁	-69.85	216.44	-2484.999813	-2484.282656	-2484.233480	-2484.372251	5.75	5.55	5.03	6.83
GS ₂	-70.32	292.82	-2485.005972	-2484.288132	-2484.238297	-2484.379928	1.89	2.11	2.01	2.01
TS ₂	-70.41	347.01	-2485.001852	-2484.284795	-2484.235586	-2484.374735	4.47	4.21	3.71	5.27
C3 GS ₁	-121.28	121.21	-2255.973714	-2255.321410	-2255.276831	-2255.406096	0.00	0.00	0.00	0.00
TS ₁	-121.24	214.87	-2255.963342	-2255.311860	-2255.267906	-2255.396296	6.50	5.99	5.69	6.15
GS ₂	-119.54	289.28	-2255.972864	-2255.320652	-2255.276018	-2255.404949	0.53	0.48	0.52	0.72
TS ₂	-121.64	353.48	-2255.965306	-2255.313594	-2255.269723	-2255.396658	5.27	4.90	4.53	5.92

Table 2- CHELPG charges calculated with B3LYP/6-31G* basis-set

Molecule	CHELPG Charges			
	=O	-OH	O32	O33
Curcumin	-0.595*	-0.579*		
A1	-0.584	-0.572	-0.553	-0.544
A2	-0.594	-0.576		
A3	-0.597	-0.569		
C1	-0.591	-0.571	-0.532	-0.534
	-0.646 (w)	-0.600 (w)	-0.572 (w)	-0.573 (w)
	-0.591 (m)	-0.571 (m)	-0.533 (m)	-0.534 (m)
	-0.623 (a)	-0.587(a)	-0.554 (a)	-0.556 (a)
	-0.623 (d)	-0.587 (d)	-0.555 (d)	-0.556 (d)
C2	-0.600	-0.580		
	-0.641 (w)	-0.595 (w)		
	-0.639 (m)	-0.594 (m)		
	-0.620 (a)	-0.584 (a)		
	-0.620 (d)	-0.584 (d)		
C3	-0.601	-0.582		
	-0.654 (w)	-0.608 (w)		
	-0.601 (m)	-0.582 (m)		
	-0.632 (a)	-0.596 (a)		
	-0.632 (d)	-0.598 (d)		

*Values taken from Ref 15. Values calculated in *vacuum* if not specified, (w) water, (m) MeOH, (a) ACN, (d) DMSO.

Table 3- Calculated averaged GIAO magnetic isotropic shielding tensors ($\bar{\sigma}_{\text{calc}}$) for **C1**, **C2** and **C3** in *vacuum* (v), MeOH (m) and DMSO (d).

¹³ C	C1			C2			C3		
	v	m	d	v	m	d	v	m	d
1	88.34	87.94	88.01	88.5	88.19	88.29	88.75	88.64	88.62
2	17.99	17.36	17.65	18.13	17.46	17.77	18.14	17.54	17.82
3	72.92	72.8	72.91	73.34	73.18	73.37	74.28	74.47	74.47
4	54.21	53.84	54.01	54.69	54	54.2	55.27	54.56	54.82
5	62.48	63.47	63.29	64.33	64.36	64.45	66.69	67.35	67.23
6	73.19	73.98	73.96	79.16	77.99	78.37	60.88	60.51	60.69
7	45.32	46.03	45.79	44.92	44.85	44.83	76.35	76.59	76.57
8	49.42	48.2	48.58	48.22	48.5	48.41	36.48	35.8	36.03
9	71.79	71.02	70.95	68.91	69.3	69.1	78.25	77.66	77.72
10	81.35	79.7	80.11	78.51	77.95	78.11	70.32	69.18	69.41
11	84.48	85.92	85.26	89.05	89.5	89.35	86.84	87.8	87.33
12	115.66	116.23	115.72	115.9	116.54	115.88	116.26	116.88	116.26
13	114.94	115.9	115.4	113.79	114.9	114.23	114.3	115.37	114.81
14	119.61	120.01	119.61	119.83	120.26	119.81	120.2	120.63	120.2
15	114.05	115.18	114.52	114.92	116.03	115.35	113.73	114.89	114.26
16	126.04	126.7	126.47	126.08	126.87	126.56	125.87	126.58	126.31
¹ H									
1	27.27	26.76	26.96	27.22	26.74	26.94	27.28	26.79	26.99
3	26.05	25.64	25.82	26.02	25.63	25.82	26.08	25.7	25.86
4	24.85	24.85	24.9	24.87	24.8	24.86	24.85	24.83	24.89
6	25.57	25.42	25.57	25.89	25.52	25.7	25.1	24.89	25.01
7	/	/	/	/	/	/	25.16	25.06	25.13
9	25.19	24.91	25.03	25.16	25.01	25.12	25.34	25.06	25.18
10	25.22	24.89	25.01	24.97	24.72	24.83	24.61	24.32	24.43
11	27.82	26.98	27.53	26.89	26.73	26.86	27.36	26.69	27.15
12	28.49	28.23	28.47	28.43	28.21	28.47	28.39	28.18	28.42
13	28.6	28.19	28.44	28.7	28.28	28.57	28.6	28.17	28.43
14	28.2	28.03	28.22	28.21	28.04	28.25	28.2	28.04	28.24
15	28.94	28.37	28.69	29.09	28.53	28.88	28.87	28.27	28.6
16	28	27.86	27.9	28.16	28	28.06	28.01	27.85	27.9
16	28.14	28.12	28.14	28.41	28.39	28.42	28.22	28.2	28.23

Table 4-Experimental (δ_{exp}) and predicted ($\delta_{\text{pred}} = a \cdot \bar{\sigma}_{\text{calc}} + b$) ^{13}C chemical shifts (ppm) for **C1**, **C2** and **C3** in *vacuum* (v), MeOH (m) and DMSO (d).

	C1						C2						C3					
	δ_{exp} (m)	δ_{pred} (v)	δ_{pred} (m)	δ_{exp} (d)	δ_{pred} (v)	δ_{pred} (d)	δ_{exp} (m)	δ_{pred} (v)	δ_{pred} (m)	δ_{exp} (d)	δ_{pred} (v)	δ_{pred} (d)	δ_{exp} (m)	δ_{pred} (v)	δ_{pred} (m)	δ_{exp} (d)	δ_{pred} (d)	δ_{exp} (m)
1	102.80	101.85	102.50	101.71	103.19	103.62	102.80	102.08	102.56	101.32	103.50	103.76	102.8	102.4	102.8	101.74	103.82	104.01
2	185.40	184.41	184.20	183.50	180.20	180.27	185.60	184.88	184.43	183.68	180.57	180.57	185.6	186.8	186.1	183.57	181.87	181.69
3	124.50	119.95	120.04	122.77	120.07	120.07	124.50	119.92	119.89	122.89	120.11	120.01	124.5	119.7	119.5	122.81	119.81	119.54
4	142.10	141.90	141.98	140.56	140.55	140.66	142.10	141.86	142.12	140.69	140.53	140.89	142.1	142.4	142.6	140.31	140.82	141.10
5	132.60	132.20	131.22	129.54	131.50	130.55	132.10	130.52	130.25	128.91	129.97	129.73	131.6	128.8	128.0	128.78	128.20	127.48
6	116.20	119.63	118.83	121.45	119.78	118.92	112.10	113.07	114.07	111.60	113.73	114.57	131.6	135.7	135.7	130.32	134.62	134.66
7	147.70	152.34	151.53	147.27	150.28	149.61	149.60	153.36	152.99	149.47	151.23	151.10	118.9	117.2	117.0	116.94	117.52	117.24
8	149.40	147.53	148.29	147.53	145.80	146.57	150.10	149.47	148.84	148.85	147.61	147.20	161.6	164.9	164.7	159.5	161.60	161.71
9	118.80	121.27	122.31	116.31	121.31	122.20	117.30	125.13	124.83	115.42	124.96	124.67	118.9	115.0	115.7	116.94	115.42	115.97
10	122.80	110.06	111.67	114.98	110.84	112.22	122.50	113.84	114.37	122.83	114.44	114.85	131.6	124.4	125.4	130.32	124.19	125.09
11	96.30	106.38	105.70	101.58	107.42	106.61	99.40	101.43	101.32	99.97	102.90	102.61	96.5	104.7	104.4	100.34	105.93	105.43
12	68.10	69.79	70.34	76.96	73.28	73.43	68.10	69.84	70.52	73.52	73.50	73.71	68.4	69.5	70.3	73.55	73.41	73.69
13	71.40	70.64	70.73	69.92	74.07	73.78	70.50	72.32	72.44	77.23	75.81	75.51	71.2	71.9	72.1	76.98	75.57	75.28
14	65.00	65.16	65.81	73.42	68.96	69.19	66.20	65.22	65.95	69.97	69.19	69.43	66.7	64.8	65.7	70.06	69.05	69.37
15	70.10	71.68	71.74	75.93	75.05	74.74	69.70	71.00	71.14	77.51	74.57	74.29	68.7	72.6	72.7	77.52	76.20	75.89
16	59.20	57.61	57.86	60.80	61.92	61.72	59.20	57.86	58.12	61.14	62.35	62.08	58.3	58.0	58.5	61.07	62.78	62.67
a		-1.174	-1.161		-1.095	-1.089		-1.177	-1.161		-1.095	-1.089		-1.195	-1.176		-1.105	-1.097
b		205.52	204.69		199.90	199.50		206.21	205.06		200.42	199.93		208.51	207.09		201.92	201.24
R ²		0.9834	0.9878		0.9905	0.9915		0.9906	0.9917		0.9879	0.9882		0.9896	0.9911		0.9933	0.9939

Table 5- Experimental (δ_{exp}) and predicted ($\delta_{\text{pred}} = a \cdot \bar{\sigma}_{\text{calc}} + b$) ^1H chemical shifts (ppm) for **C1**, **C2** and **C3** in *vacuum* (v). MeOH (m) and DMSO (d).

^1H	C1						C2						C3					
	δ_{exp} (m)	δ_{pred} (v)	δ_{pred} (m)	δ_{exp} (d)	δ_{pred} (v)	δ_{pred} (d)	δ_{exp} (m)	δ_{pred} (v)	δ_{pred} (m)	δ_{exp} (d)	δ_{pred} (v)	δ_{pred} (d)	δ_{exp} (m)	δ_{pred} (v)	δ_{pred} (m)	δ_{exp} (d)	δ_{pred} (d)	δ_{pred} (m)
1	6.01	5.05	5.27	6.12	4.96	5.17	6.02	5.07	5.31	6.13	5.03	5.25	6.01	4.98	4.97	6.11	4.89	5.09
3	6.63	6.40	6.58	6.75	6.39	6.54	6.72	6.38	6.56	6.87	6.44	6.57	6.69	6.31	6.26	6.83	6.31	6.44
4	7.53	7.74	7.50	7.52	7.80	7.64	7.6	7.63	7.50	7.6	7.79	7.71	7.62	7.67	7.40	7.61	7.76	7.60
6	7.14	6.94	6.83	7.13	6.96	6.84	7.12	6.52	6.69	7.38	6.59	6.71	7.14	7.40	7.25	7.7	7.46	7.46
7	/	/	/	/	/	/	/	/	/	/	/	/	7.61	7.33	7.11	7.09	7.39	7.32
9	7.20	7.36	7.43	7.13	7.40	7.48	7.18	7.31	7.26	7.13	7.45	7.40	7.60	7.13	7.05	7.09	7.18	7.26
10	7.07	7.32	7.45	7.2	7.37	7.51	7.18	7.52	7.59	7.26	7.67	7.74	7.14	7.94	7.92	7.7	8.04	8.15
11	4.97	4.44	5.01	4.81	4.31	4.49	4.98	5.43	5.32	4.99	5.42	5.34	4.98	4.90	4.79	4.96	4.79	4.90
12	3.53	3.69	3.55	3.30	3.52	3.37	3.53	3.75	3.65	3.27	3.61	3.44	3.52	3.76	3.33	3.27	3.58	3.38
13	3.47	3.57	3.60	3.18	3.40	3.40	3.48	3.45	3.57	3.28	3.29	3.32	3.47	3.52	3.30	3.29	3.33	3.37
14	3.44	4.02	3.79	3.32	3.87	3.67	3.43	3.99	3.84	3.17	3.87	3.70	3.42	3.97	3.55	3.17	3.80	3.60
15	3.45	3.19	3.39	3.36	3.00	3.10	3.45	3.03	3.28	3.34	2.83	2.95	3.45	3.22	3.11	3.37	3.01	3.17
16	3.90	4.24	3.98	3.72	4.10	4.05	3.89	4.04	3.88	3.67	3.93	3.92	3.91	4.18	3.93	3.69	4.03	4.00
16'	3.71	4.08	3.68	3.48	3.94	3.76	3.71	3.77	3.44	3.45	3.63	3.50	3.71	3.94	3.55	3.46	3.78	3.61
a		-1.110	-1.168		-1.175	-1.197		-1.091	-1.131		-1.175	-1.183		-1.107	-1.150		-1.181	-1.196
b		35.324	36.527		37.003	37.442		34.772	35.537		37.019	37.1198		35.183	36.005		37.103	37.359
R ²		0.9399	0.9718		0.9295	0.9553		0.9232	0.9524		0.9186	0.9465		0.9362	0.9479		0.9399	0.9611

Table 6- Uv-vis band maximum position (nm) in different solvents for compounds **C**.

	Vacuum	H ₂ O		MeOH		ACN		DMSO	
	calc	exp	calc	exp	calc	exp	calc	exp	calc
C1	402	414	423	411	422	405	419	423	421
C2	413	413	432	411	432	413	428	425	431
C3	403	408	425	406	425	405	420	416	423

For Peer Review

Caption of Figures

Figure 1: General structure of the studied curcumin glucosyl derivatives.

Figure 2: ΔG for compounds **A1**, **A2** and **A3** as a function of the rotational dihedral angle ϕ .

Figure 3: Final optimized structures of **A** compounds at B3LYP/6-31G* level at GS₁ and GS₂ states. The hydrogen interaction is represented by dots.

Figure 4: Top view of **C2** optimized structures at B3LYP/6-31G* level showing the different sugar spatial positions with respect to curcumin planar skeleton and their total energies (a.u.).

Figure 5: Representation of HOMO and LUMO orbital density for **A** and **C** series at B3LYP/6-31G* level.

Figure 6: Molecular electrostatic maps in *vacuum* of compounds **A** and **C** in their GS₁ states at B3LYP/6-31G* level.

Figure 7: ¹H NMR spectrum of **C1** in DMSO-*d*₆ (* residual DMSO)

Figure 8: Plots of DMSO-*d*₆ vs. MeOD experimental ¹H (**A**) and ¹³C (**B**) chemical shifts (δ) for glucosyl-curcuminoids: **C1** (∇), **C2** (\square) and **C3** (\circ).

Figure 9: Plot of ¹H and ¹³C δ_{exp} vs. $\bar{\sigma}_{\text{calc}}$ for **C1**. Solid circle is referred to H-1 proton; dotted circle highlights anomeric proton (H-11).

Figure 10: Correlation between experimental and B3LYP/6-311G* in *vacuum* calculated wavenumbers for **C1**. Equation: $\bar{\nu}_{\text{exp}} = a \cdot \bar{\nu}_{\text{calc}}$; $a = 0.9991$, $R^2 = 0.9983$.

Figure 1

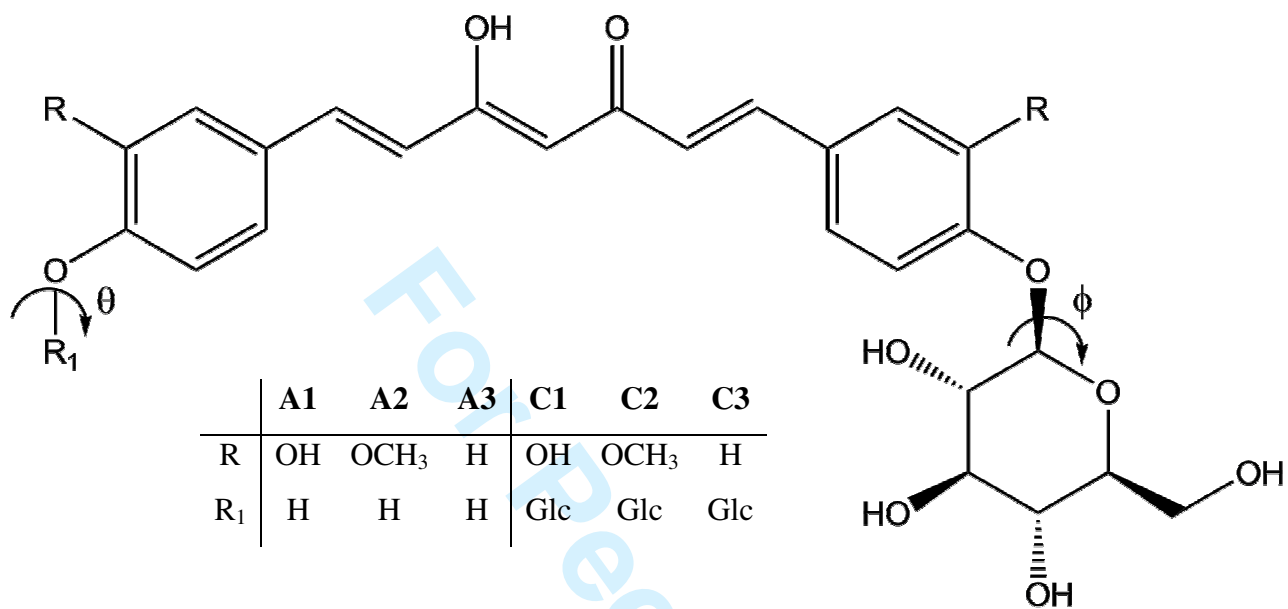


Figure 2

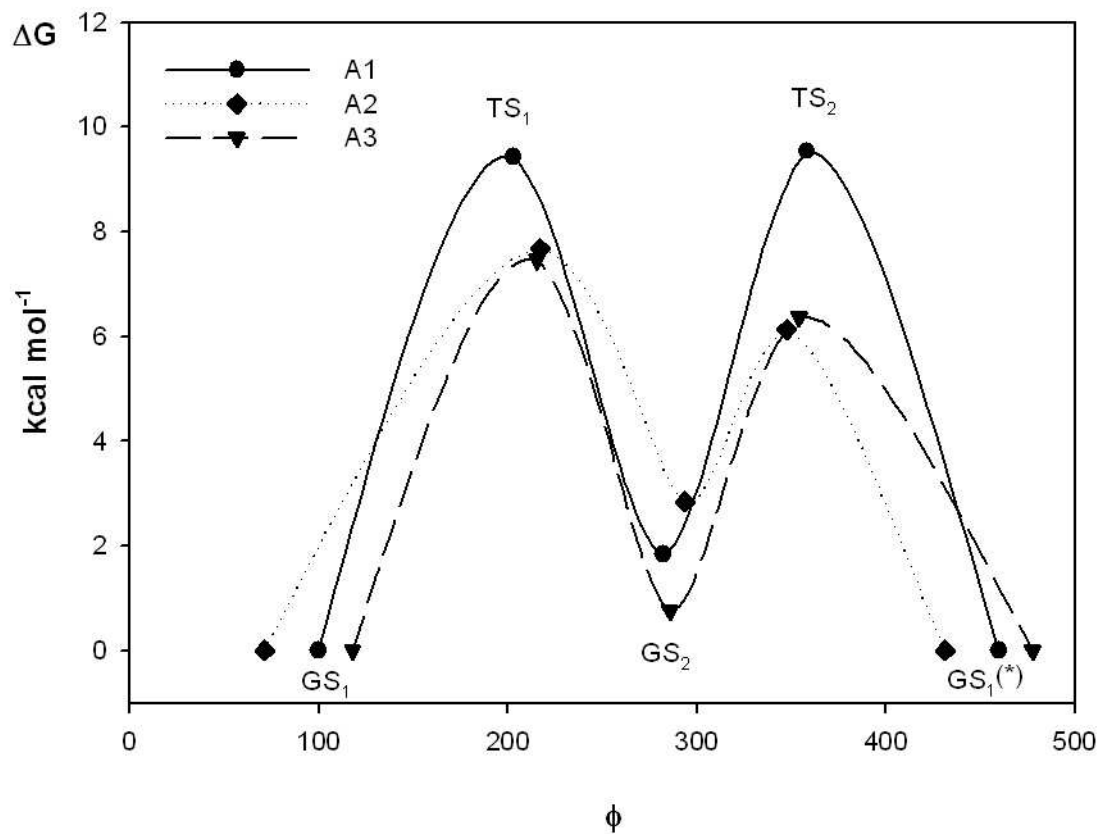


Figure 3

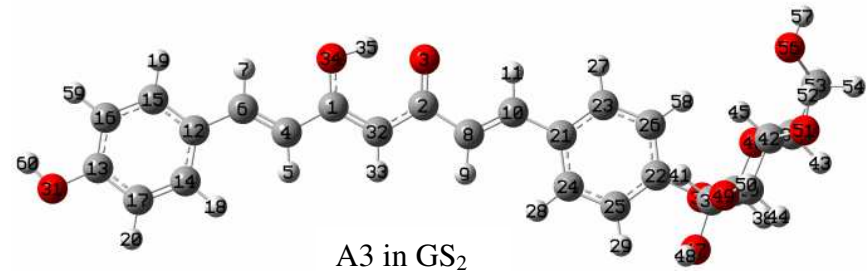
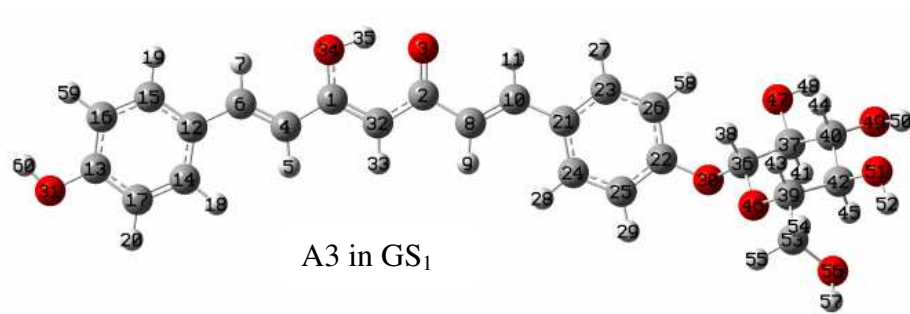
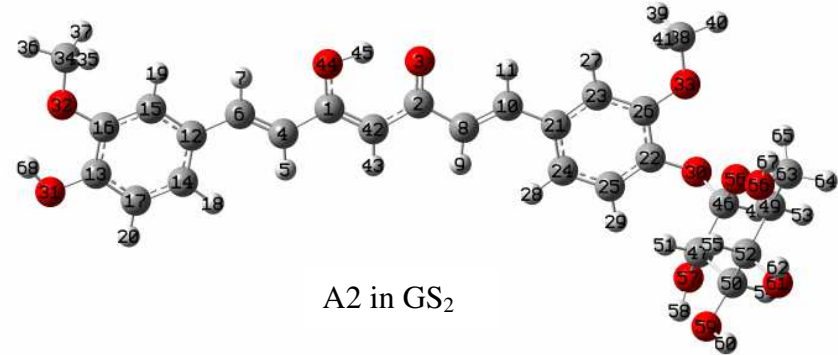
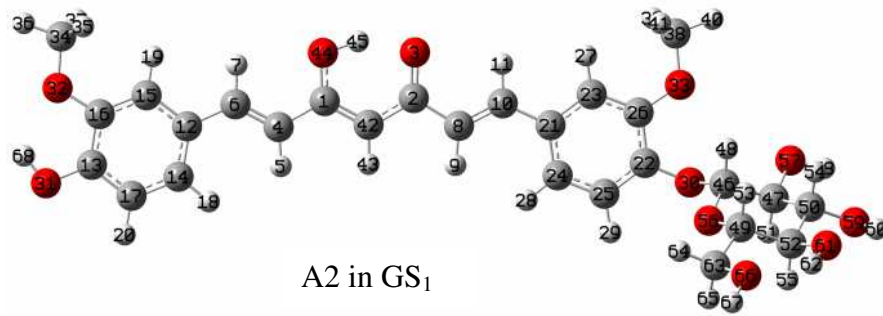
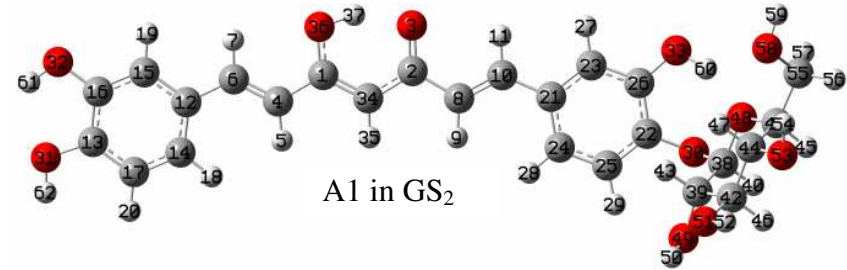
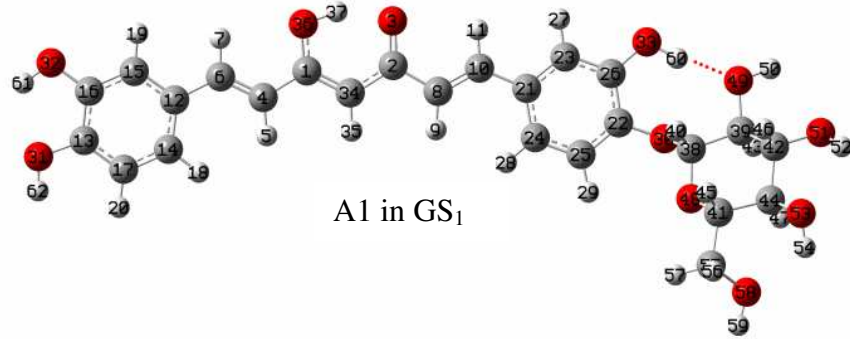
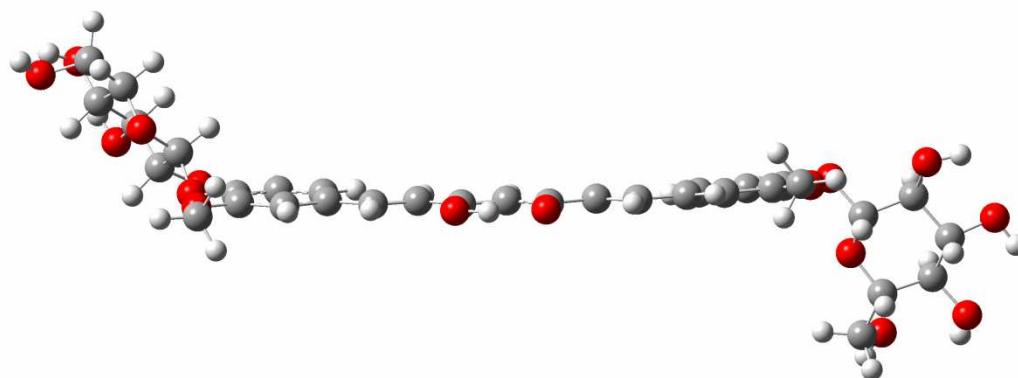
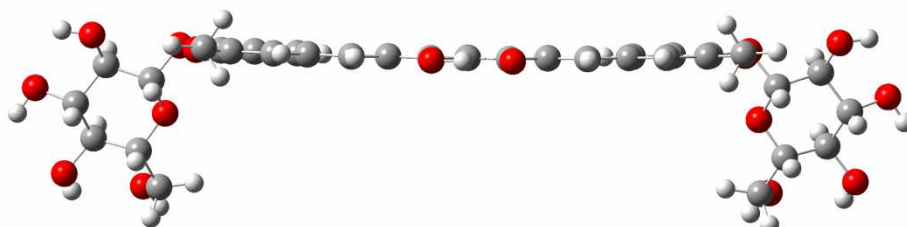


Figure 4



sin-anti configuration $E = -2485.008088$ a.u.



sin-sin configuraton $E = -2485.008984$ a.u.

Figure 5

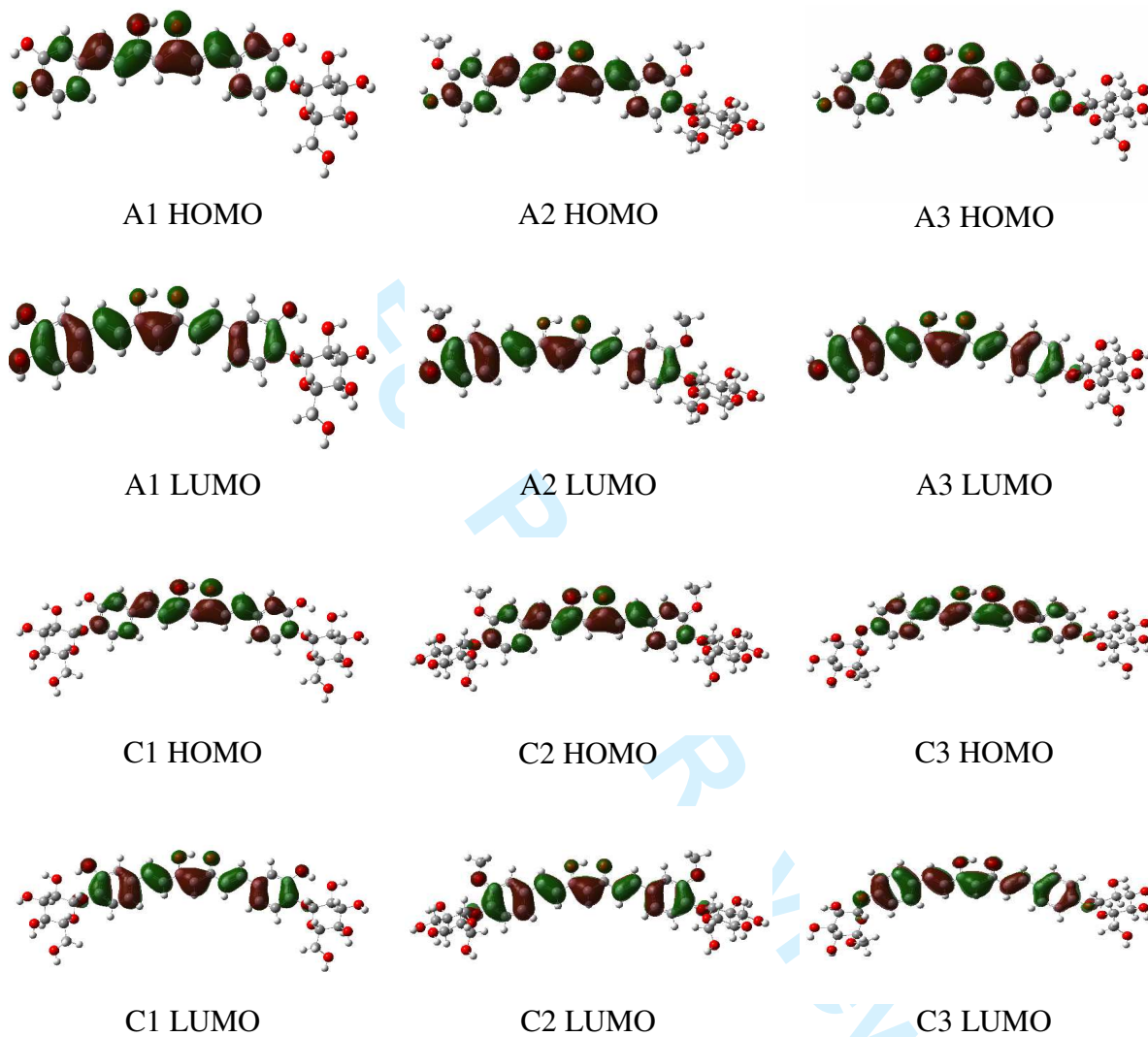


Figure 6

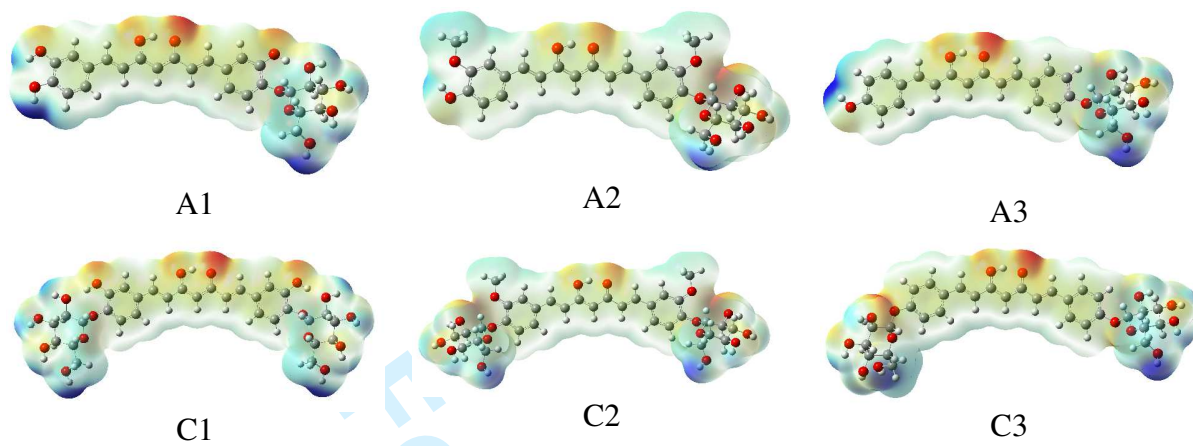


Figure 7

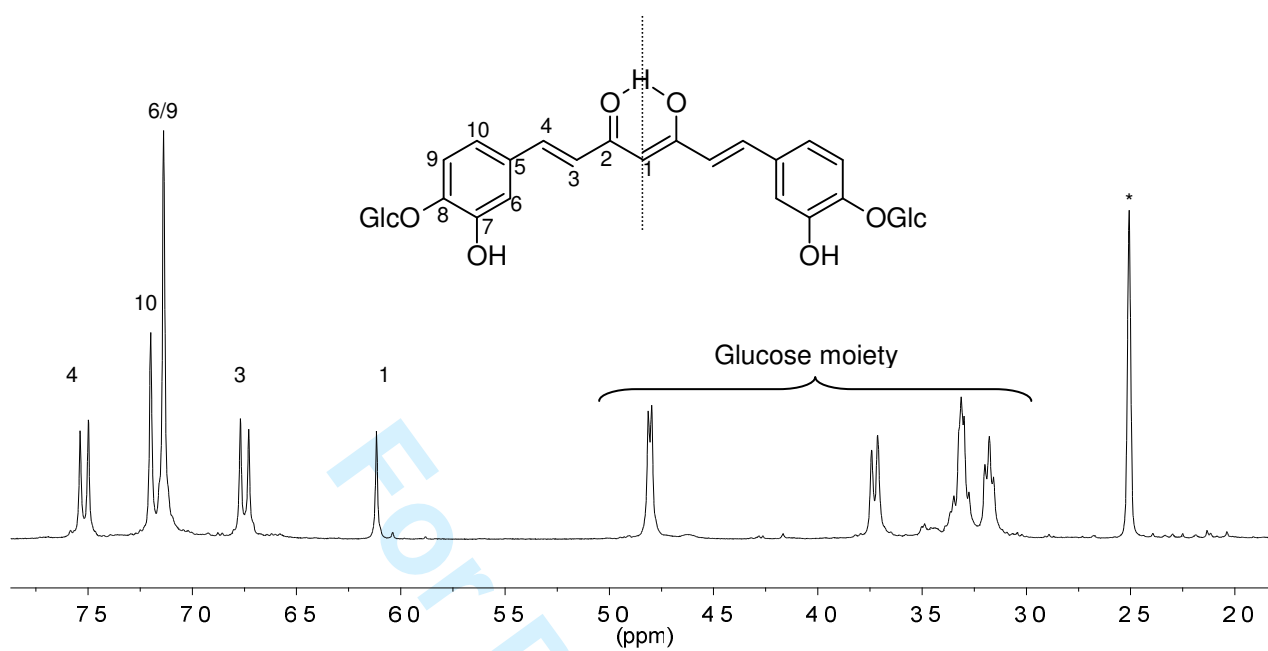


Figure 8

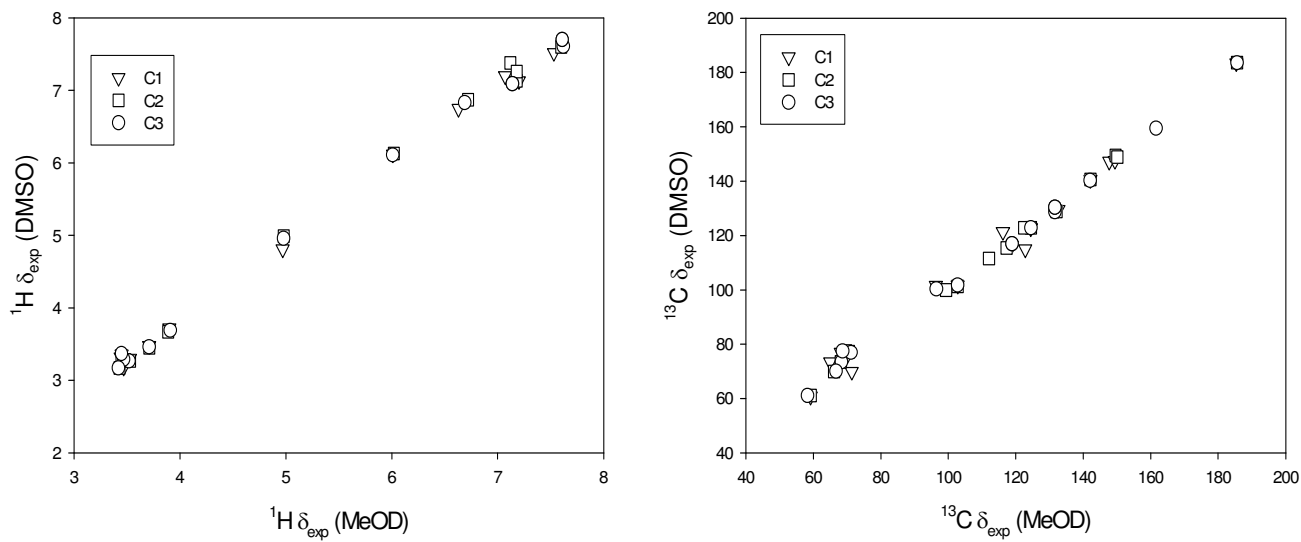


Figure 9

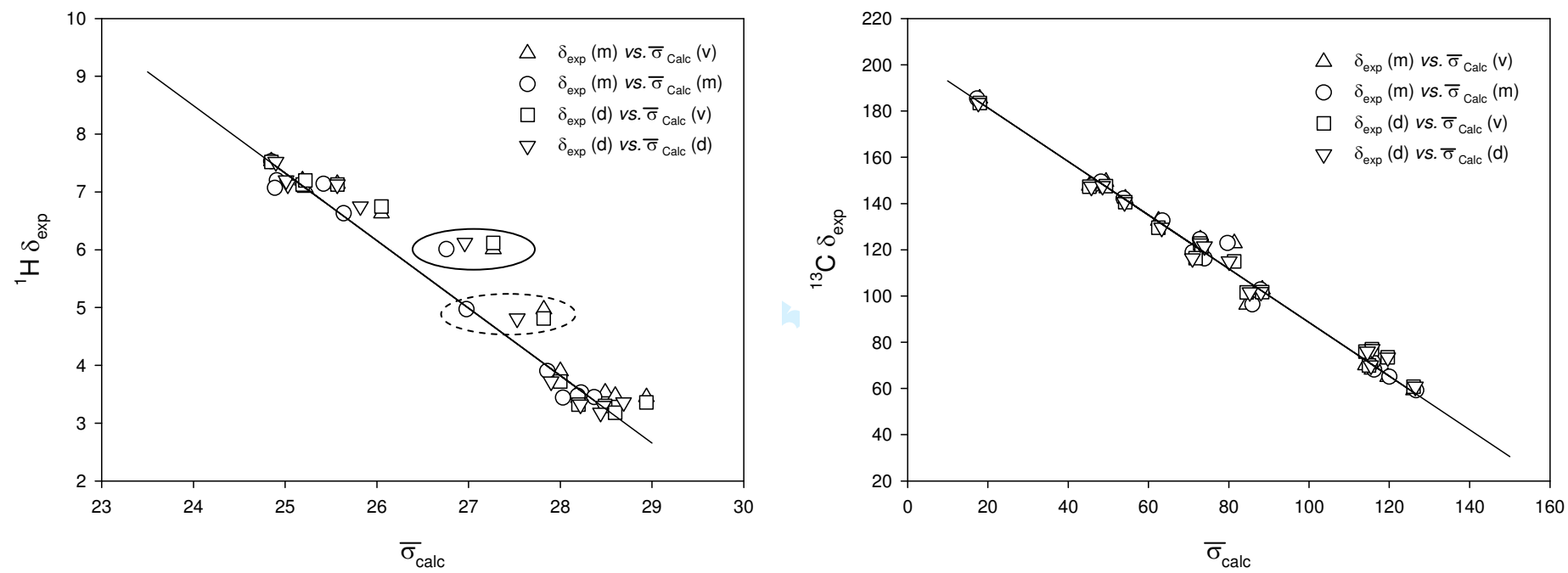
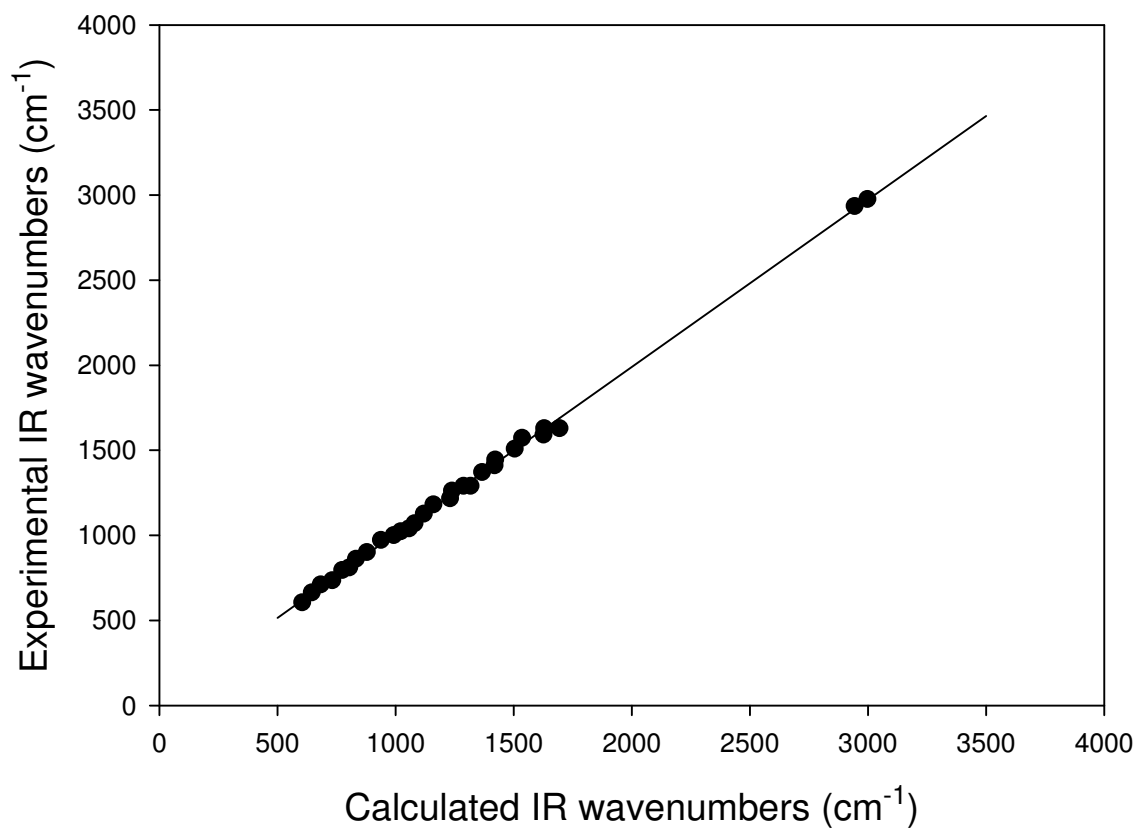


Figure 10



Review